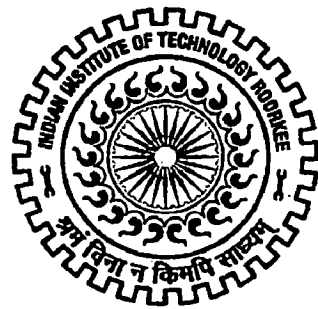# SIMULATION OF VARIABLE SPEED SMALL HYDRO POWER PLANT

A DISSERTATION

Submitted in partial fulfillment of the
requirements for the award of the degree
of
MASTER OF TECHNOLOGY
in
ALTERNATE HYDRO ENERGY SYSTEMS

By

MANJUL TRIPATHI

ALTERNATE HYDRO ENERGY CENTRE
INDIAN INSTITUTE OF TECHNOLOGY ROORKEE
ROORKEE - 247 667 (INDIA)
JUNE, 2007

INDIAN INSTITUTE OF TECHNOLOGY ROORKEE, ROORKEE

CANDIDATE'S DECLARATION

I hereby declare that the work presented in the dissertation entitled "**Simulation of Variable Speed Small Hydro Power Plant**" submitted in partial fulfillment of the requirements for the award of degree of **Master of Technology** in **Alternate Hydro Energy Systems** in the Alternate Hydro Energy Centre, Indian Institute of Technology Roorkee, is an authentic record of my own work carried out from July 2006 to June 2007 under the guidance and supervision of **Dr. J. D. Sharma**, Professor, Electrical Engg. Department and **Dr.R.P. Saini**, Senior Scientific officer, Alternate Hydro Energy Centre.
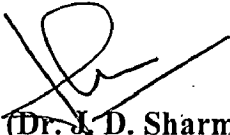
I also declare that I have not submitted the matter embodied in the dissertation for award of any other degree or diploma.
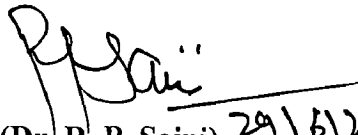
Date: June , 2007

Place: Roorkee

(Manjul Tripathi)

This is to certify that the above statement made by the candidate is correct to the best of our knowledge.

(Dr. J. D. Sharma)

Professor

Electrical Engg. Department
Indian Institute of Technology,
Roorkee

(Dr. R. P. Saini)

Associate Professor

Alternate Hydro Energy Center
Indian Institute of Technology,
Roorkee

i

ACKNOWLEDGEMENT

I wish to express my profound sense of gratitude to **Dr. J. D. Sharma**, Professor, Electrical Engineering Department, Indian Institute of Technology Roorkee for the valuable guidance and continuous inspiration for completing the aforesaid dissertation work.

I am highly indebted to **Dr. R. P. Saini** ,Associate Professor, Alternate Hydro Energy Centre, Indian Institute of Technology, Roorkee for the guidance ,encouragement and cooperation during the dissertation work.

I also express my sincere regards to **Shri Arun Kumar**, Head, Alternate Hydro Energy Centre, Indian Institute of Technology, Roorkee for his immense support, encouragement, and inspiration.

I also express thanks to my parents who have always been source of inspiration for me . And at last I would like to mention omnipresent and omnipotent God who improves my skill and makes me compatible to complete this work.

Date: June   , 2007

Place: Roorkee

(Manjul Tripathi)

ABSTRACT

This work deals with the simulation of a grid connected variable speed Small Hydro Power Plant. When the SHP plants face a large variation of discharge throughout the year, it is advantageous to use Variable Speed Generation. With the variation of discharge efficiency decreases very sharply at constant speed operation.. By variable speed operation high efficiency gain can be achieved at part load conditions. Potential advantages of variable speed hydroelectric generation are discussed in this work. Some general aspect of efficiency gain in turbines and improvement in plant operation are analysed. Variation of active and reactive power at sub synchronous and super synchronous speeds are also analyzed. Doubly Fed Induction Generator (DFIG) is used as variable speed generator. At super synchronous speed rotor can also deliver power to the grid thus can supply more than rated load without overheating. AC/DC/AC convertor is used with DFIG. Rating of convertor used in DFIG depends upon its maximum slip ($\pm$ 30%), hence its rating is approximately one third of that would be used in Squirrel Cage Induction Generator . Control schemes for grid side convertor and rotor side convertor are discussed. Responses are obtained under different operating conditions.

CONTENTS

List OF FIGURES

INTRODUCTION AND LITERATURE SURVEY

Hydro power is an important source of alternate energy in India. Availability of small streams is in plenty in hilly areas and large canal networks in planes provide good potential of small hydro in both areas. Estimated capacity of small hydro in India is more than 15,000 MW. Recently due to crisis of energy, harnessing of small hydro potential is attracting attention in India and other countries. No water storage is required in these schemes so they are easy to implement.

1.1 Small Hydro Power Plant

There are two schemes of Small Hydro Power Plants.

(1) Run of River Based SHP

(2) Canal Based SHP

1.1.1 Run of River based Scheme

These schemes are for hilly areas where small streams are found .Head is high and discharge is low. This scheme is shown in Fig. 1.1. In this scheme water is tapped from the river through diversion weir. It is carried to the forbay and desilting tank through power channel. And from for bay to Powerhouse it comes through the penstock. From penstock it goes to turbine and after that through tailrace it again comes in to river.

1.1.2 Canal Based Schemes

Canal based schemes are for plane areas where canal networks are found. This scheme is shown in Fig. 1.2. These are low head and high discharge schemes. Water is diverted to
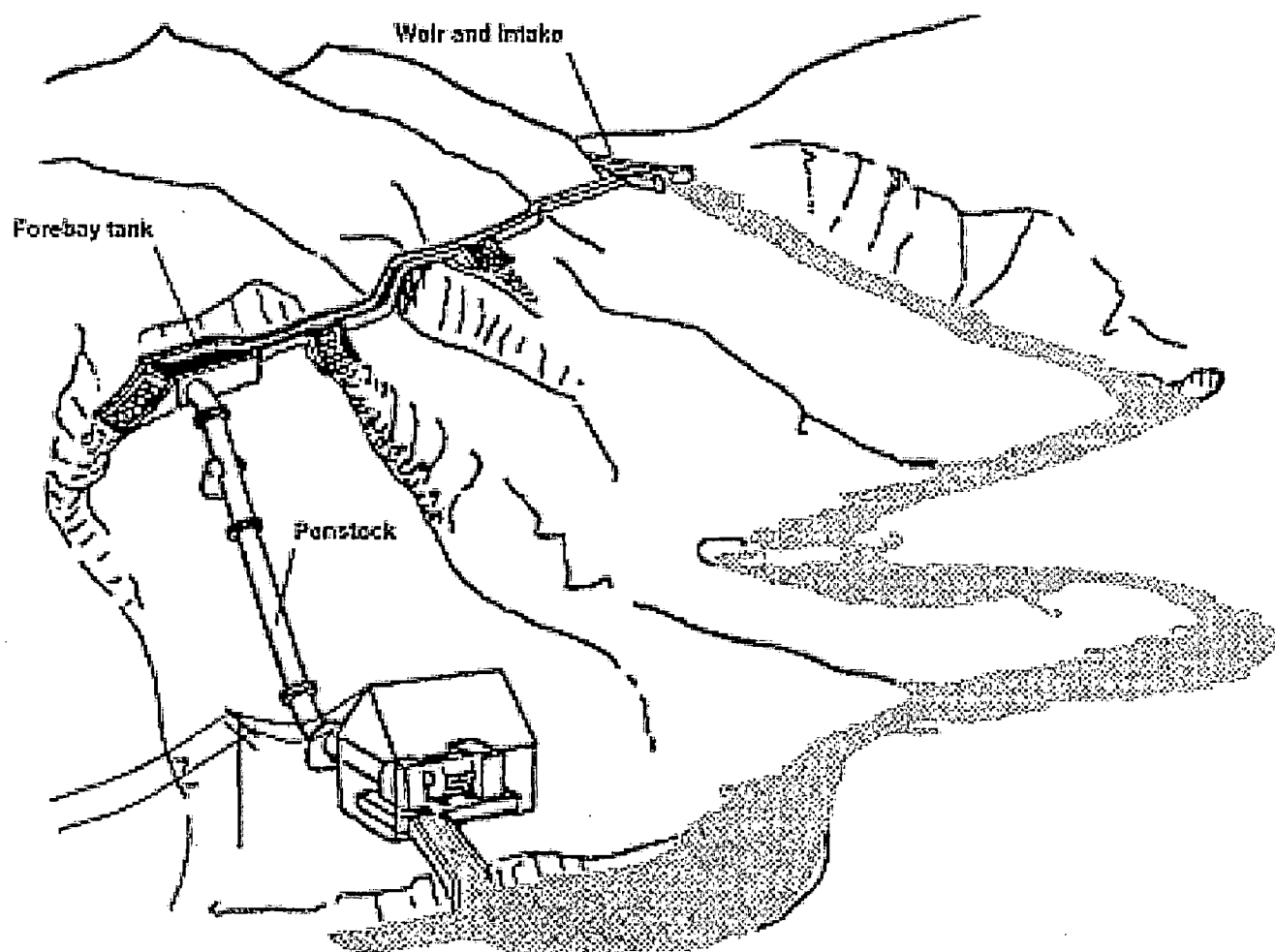
Fig. 1.1 A view of Small Hydro Power Plant (Run of River Scheme)

power channel through barrage on the main canal. Then it comes to power house in turbine. And then through tail race it again comes to canal.

Fig 1.2 Canal Based Scheme

1.2 Variable speed Turbine

Now a days variable speed operation is attracting more attention in hydro power generation. Similar to aerodynamics of wind energy converters, advantage of variable speed operation (VSO) of Hydro Turbine can be expected from simple fluid dynamics consideration. For low head sites the combination of variable speed operation with propeller turbines is most promising. The variation of runner speed with the speed of the fluid and so with the discharge allows widening of typically small range of high efficiency of propeller turbine [1],[2]. In conventional scheme when a hydro turbine is coupled to a synchronous machine which is directly connected to electric grid speed

3

variation is not possible. At fixed speed operation any head and discharge variation involves an important decrease in efficiency.

Unlike a double regulated Kaplan turbine, VSO of a propeller turbine does not allow for the same high efficiency over a wide range of operation. But still the same energy production can be obtain at lower investment cost with a VSO system and so lower specific cost for the electricity produced at the plant. In addition the variation of flow with speed allows to control the discharge over a wide operating range only by variation of speed. Depending on the site specific hydraulic conditions this can allow to have fixed guide vane as well.

1.3 Variable Speed Generator (Induction Generator)

The operation of an induction machine at super-synchronous speeds as a grid connected generator is well known. In the conventional use of a generator, the machine has a short-circuited rotor and is driven by a regulated source of mechanical power. For such applications, the induction machine has the advantage of allowing the use of a relatively simpler speed governor than that of a Synchronous generator, since the machine is able to produce electricity at a constant frequency over a limited range of shaft speed variations [7].

For variable speed generation in hydro and wind energy applications, various induction generator schemes have been proposed .The variable speed, constant voltage, constant frequency self-excited induction generator for autonomous systems has been widely used and largely discussed [16-19]. For grid-connection applications, the squirrel-cage induction machines are nowadays increasingly used in wind generation systems

4

since the terminal voltage and frequency controls are not required and the reactive power demand can be met by the grid.

Furthermore, when the generator is to be driven by an Hydro Turbine , it is obviously advantageous to use a wound rotor induction generator as a variable-speed constant-frequency system to maintain maximum power transfer conditions for shaft speed variations over a wide range and, hence, to maximize the annual energy production. This can be achieved by the use of a converter cascade between the slip rings terminals and the utility grid to control the rotor power. This scheme is called doubly fed induction generator (DFIG) scheme, because the power output is tapped from both the stator and the rotor circuits. Therefore, the DFIG is the only known scheme in which the generator gives more than its rated power without being overheated and the power generation can be realized in a wide range of wind speeds [20].
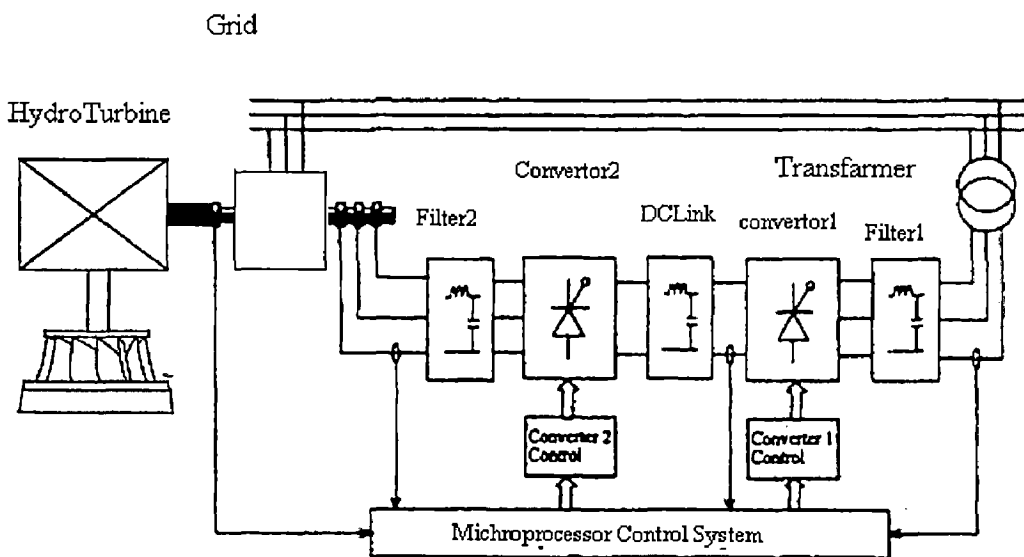
Fig. 1.3 General Structure of Doubly Fed Induction Generator

Figure 1.3 shows the schematic of the doubly fed induction generator. The general system consists of a (DFIG); two converters; one connected to the generator rotor terminal with DC link and the other to DC link with the grid through a transformer; two AC filters and one DC filter in the circuit. The type of filters depend on what type of converters are used. The rating of the converter depends on maximum slip range. It will reduce the cost of converter in comparison to full scale frequency converter scheme with squirrel cage induction generator.

Three schemes are for hydro energy conversion systems are described below .

1.3.1 Squirrel cage induction generator scheme

A squirrel-cage induction generator offers the most economical means of wind power generation to an existing power grid. This is because the generator is simple and robust, and the control system is less complicated. This kind of scheme is called Scheme 1 in Fig. 1.4 **(a)**.
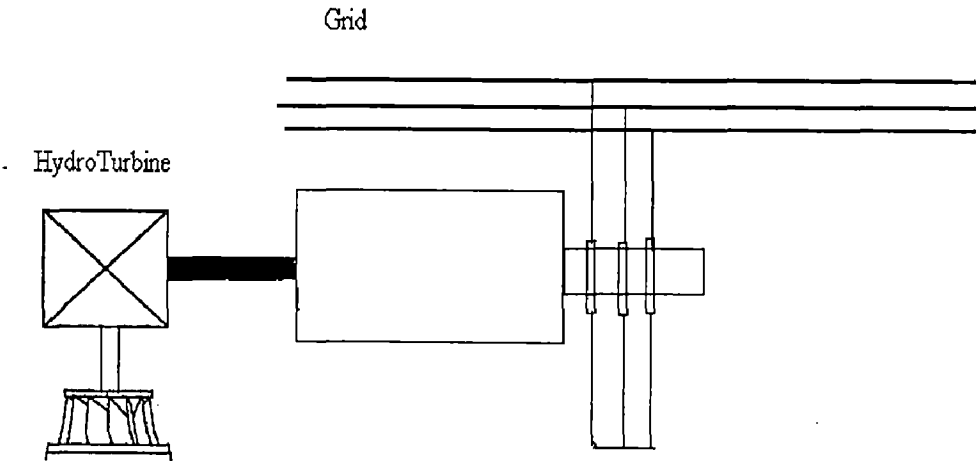
Fig. 1.4(a) Rotor wound shorted or Squirrel cage induction generator
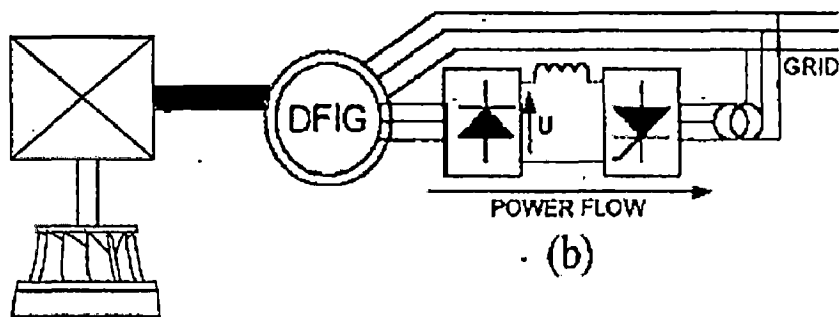
Scheme 2: A bridge diode rectifier and an SCR inverter scheme

Hydro
Turbine

Convertor 2   POWER FLOW   Convertor 1
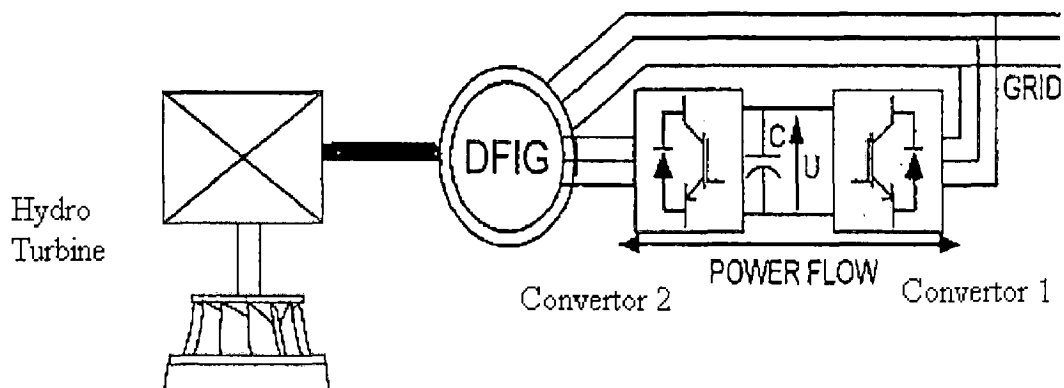
Scheme 3: Two back-to-back IGBT PWM converter scheme

Fig. 1.4 Various induction Generator Schemes

1.3.2 A bridge diode rectifier and an SCR inverter scheme

In Scheme 2 (Fig. 1.4 (b)), the DFIG, with a 3-phase diode bridge rectifier and a line commutated thyristor inverter connected between the rotor and the grid, operates only at super-synchronous speeds (- 1<s < 0) to provide the generation of electrical power from both the stator and rotor circuits. Power from the rotor, which is generated at slip frequency, is first converted to DC, then is inverted to synchronous frequency AC before being fed to the grid. The rectifier and inverter both are naturally commutated by the alternating EMF appearing at the slip-rings and supply buses. The direction of power flow through the converter is, therefore, unidirectional. The total power output of the generator can be controlled by varying the firing angle of the SCR inverter [7].

The 3-phase bridge rectifier's voltage rating is determined by the maximum working slip of the generator, because rotor EMF is proportional to slip. The current rating of the rectifier bridge is determined by the maximum rotor current corresponding to the maximum output torque. With a constant torque, the rotor current, I_r, and the air gap power, P_{ag}, are approximately constant. Maximum rotor voltage occurs at the greatest controllable slip s, when, neglecting rotor circuit loss, the converter system transfers the slip power. sp_{ag}, from the rotor to the grid system [21].

The inverter bridge is rated for the applied AC voltage and the alternating current corresponding to the maximum output torque of the generator. In order to minimize the rating of rectifier and inverter, the transformation ratios of the generator and transformer must be chosen such that the lowest controllable slip requires full inversion.

This design procedure also optimizes the power factor of system. The inverter transformer is only rated for the inverter *kVA*.

The use of this current source DC link converter has a number of disadvantages:

1. At operating speeds close to synchronous speed ($-0.2 < s < 0.2$) [2], the rotor frequency and generator EMF are both low. This condition imposes difficulties in the commutation of the diode rectifier bridge because the overlap period may be appreciably prolonged due to the small rotor EMF and relatively large rotor leakage reactance. Therefore, an extra commutation circuit is required for the operation and resulted in poor performance of the speeds.

2. This scheme requires a transformer to match the voltages between the grid and the commutated DC link and a wound rotor, which is larger and more expensive than a squirrel cage rotor.

3. The rectification and conversion processes produce non-sinusoidal rotor currents which induce associated harmonic currents in the stator winding. These harmonic currents cause additional harmonic torque and losses that reduce the machine's efficiency and affect the power quality. With additional losses in the DC link reactor and semiconductor, the generator must be derated by 10 to 15 percent in the scheme.

4. The generator can operate at super-synchronous speeds only and lacks reactive power generation capability due to the diode-bridge rectifier.

By replacing the diode-bridge rectifier with a controlled converter, a bidirectional power flow can be achieved. The details on the scheme with two SCR converters has been investigated in Reference [7].

1.3.3 Two back-to-back IGBT PWM converter scheme

The disadvantages of the naturally commutated DC-link (scheme 2) can be overcome by the use of two PWM voltage-source current-regulated inverters connected back-to-back in the rotor circuit. The characteristics of such a scheme, in which both converters are vector controlled, are as follow:

1. At the synchronous speed, the inverter connected with the rotor is working in chopping mode so that the generator can be excited by injecting DC currents in to the rotor.

2. The generator is able to operate below, above and at synchronous speed successively. The speed range is restricted only by the rotor voltage ratings of the DFIG.

3. The high switching frequency of IGBT lowers the distortion of stator, rotor, and grid currents.

4. The two IGBT converters operate as inverters to adjust both output sinusoidal currents, so the generator torque and rotor excitation can be controlled independently. The DC link capacitor smoothes the DC voltage.

5. The system power factor can be controlled by the grid-side converter or the rotor side converter, depending on operation levels and conditions.

The major benefit of this system is that the output power of the induction generator can be controlled continuously by the rotor circuit converter, which is rated at a fraction of the generator rating, thus allowing the extraction of the maximum power from the wind turbine at various wind speeds at a lower cost. The rated power of the system is determined critically by the power capability of the rotor winding and IGBT inverters. In

10

addition, this wind energy conversion scheme is viable for both wind turbine-grid system and stand alone systems, which is an attractive feature for the remote communities [8].

1.4 Power flow consideration

The direction of power flow in the induction generator operating at sub-synchronous and super-synchronous speeds as a result of rotor power control is shown in Fig. 1.5.

P_s stator terminal power

P_r - rotor terminal power

P_m - SM mechanical power

P_{og} - air gap power

P_{cs} - stator copper losses

P_{cr} - rotor copper losses

   s - slip

If the shaft power to the generator from the wind turbine is Pm, then the power crossing the air gap $P_{ag} = P_m/(1-s)$ is greater than the shaft power at sub-synchronous speeds, as shown in Fig. 1.5(a). The rotor power source, therefore, must provide a power $P_r = sP_{ag}Pr = sPg$ in addition to the total rotor copper loss P_{cu}, where P_{cu} represents the sum of losses in the rotor windings and losses in the rectifier, DC link, inverter, and transformer. The net output power into the grid is $P_o = P_s - P_r$. For super-synchronous

Ps
Pag=Pm/(1-s)

Pm

Pag>Pm

Pcus

Pcur

Pr

(a) Subsynchronous Power Generation

Ps
Pag=Pm/(1-s)

Pm

Pcus
Pag<Pm
spag
Pr

Pcur

Supersynchronous Power Generation
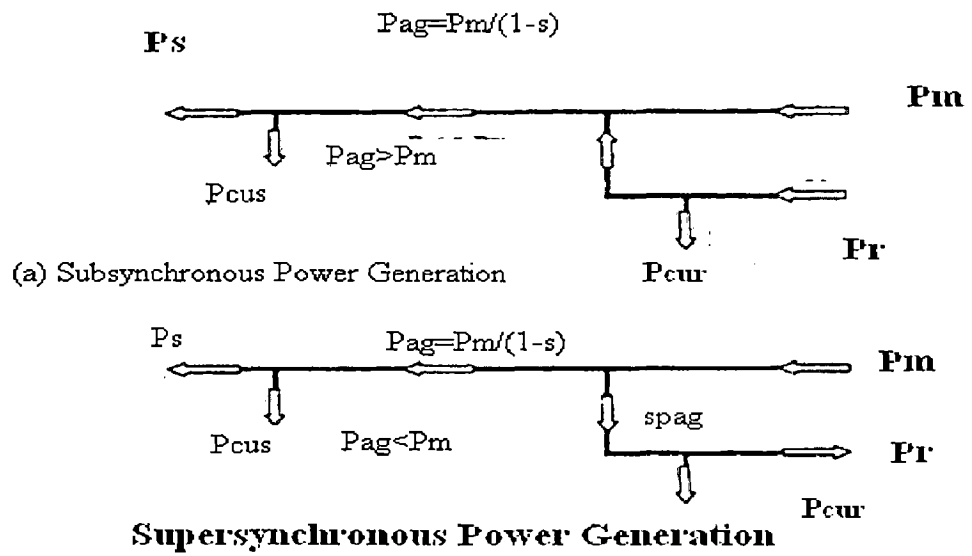
Fig. 1.5 Power flow diagram ignoring iron loss

operations, the power flow is shown in Fig. 1.5(b), in which the change in sign of slip has

been included. At this time, the power crossing the air gap P_{ag} is less than the shaft

power P_m, and the remaining energy sP, is returned via the rotor circuit to provide the

loss P_r and power Pr into the grid system. The net power output is then $P_o = P_s + P_r$

12

Literature Review

In last two decades several work have been done on variable speed operation of hydro and wind power generation. People have discussed both aspects i.e. electrical and mechanical systems related to variable speed generation. Some of those works are presented here.

1. Sheldon, L. H., [1], analyzed the effect of variable speed on Francis turbine. In that analysis, variable speed was not found to be an effective flow control mechanism .it was found, in general to increase energy production and/or reduce discharge on Francis turbine a few percent under varying head conditions. However, under the same varying conditions, it did produce a significant benefit of several percent when the Francis turbine unit was operated solely for maximum efficiency.

2. Sheldon, L. H [2], analyzed variable sped operation of fixed blade propeller turbine in constant head and gate, and comparison is made in energy production and discharge between variable and constant speed as the unit is operated under varying head conditions. A general methodology is developed to evaluate the benefits resulting in variable speed operation to any given specific turbine performance and/or site specific hydrologic operating conditions.

3. Bard, J. and Ritter, P. gives the idea of VSO of a turbine to allow the turbine speed to change with hydraulic conditions in order to maximize the turbine efficiency. In that work they described the velocity vectors at the turbine blades at design flow and for a lower flow , the guide vanes are closed and the turbine blades are turned accordingly. In case of the variable speed propeller turbine the speed is reduced in proportion with flow in such a way, that the fluid velocity vectors match the design conditions. He also

presented case study of Hydropower plant Rottenburg River Neckar, Rotenberg, Germany. He described that at part load conditions, total system efficiency improvements in the range of 10 % can be achieved.

4. Grotenburg K., Bachmann,U. [4], described the modeling of variable speed pump storage power plant units equipped with double fed induction machine drives. They investigate the dynamic interaction between large variable speed units and the interconnected power system. First, a reduced order model of the double fed machine is developed. Based on this, a systematic multivariable controller design with dead-beat controller approach and terminal voltage compensation is carried out.

5. Jes'us Fraile-Ardanuy, Jos'e Rom'an Wilhelmi, Jos'e Jes'us Fraile-Mora, *Senior*, and Juan Ignacio P'erez. [5] analyzed some general aspects concerning the efficiency gains in turbines and the improvements in plant operation. The main results of measurements on a test loop with an axial-flow turbine are reported. Also, they described the control scheme implemented, which is based on artificial neural networks. The operation of a run-of-the-river small hydro plant has been simulated for several years. Substantial increases in production with respect a fixed-speed plant have been found.

6. Soens, J., Karel de Brabandere, Driesen,J., Belmans. R., [6], analyzed the electric loading of the rotor windings and the frequency converter as a function of speed range and stator reactive power. This is done using an equivalent circuit of the doubly fed machine. In a next step, a dynamic simulation of a doubly fed induction generator is made. This allows assessing the impact of a grid disturbance on the machine behavior

7. Cadirci, I. Ermiq, M., [7] analyzed steady-state behavior of a wound-rotor induction generator operated at varying shaft speeds in the sub synchronous and super

synchronous regions, by control of both the magnitude and direction of slip power. An optimum control strategy, which maximizes the total electrical power output of the double output induction generator is determined. with naturally commutated converters. The limitations of naturally commutated convertor circuits and their effects on the output power characteristic of the system are also discussed. A comparison is made among optimised versions. of alternative induction generator schemes used in wind-energy conversion systems, on the bases of annual energy production and transfer characteristic for the same site and turbine

8. Pena, R., Clare, J.C., Asher, G.M [8] in their work described the engineering and design of a doubly fed induction generator (DFIG), using back-to-back PWM voltage-source converters in the rotor circuit. A vector-control scheme for the supply-side PWM converter results in independent control of active and reactive power drawn from the supply, while ensuring sinusoidal supply currents. Vector control of the rotor-connected converter provides for wide speed-range operation. the vector scheme is embedded in control loops which enable optimal speed tracking for maximum energy capture from the grid connected wind farm.

9. Fraile-Ardanuy, J., Wilhelmi, J.R., J. Fraile-Mora, J. I. Pérez and I. Sarasúa [9]. In the simulation of adjustable speed hydro plants They implemented optimum speed for actual working conditions means of an appropriate control system. This process gives rise to dynamic changes in operation variables. In their work, a speed control of run-of-river adjustable speed hydro plant is presented.

VARIABLE-SPEED HYDRAULIC TURBINES

Generally the potential advantages of variable speed operation are found in

Francis turbines with high specific speed and in Kaplan or propeller turbines [12].

2.1 Francis Turbines

In Fig. 2.1, the hill curves of a typical Francis turbine are represented in unit values

$n_1 - Q_1$. From this figure, it is clear that the efficiency drops appreciably if n_1 or Q_1

deviates from the optimal values. In a constant speed turbine, this occurs when the net

head H, or the discharge Q, change, as shown in (2.1).

$$n = n_1 \sqrt{H}/D_1$$

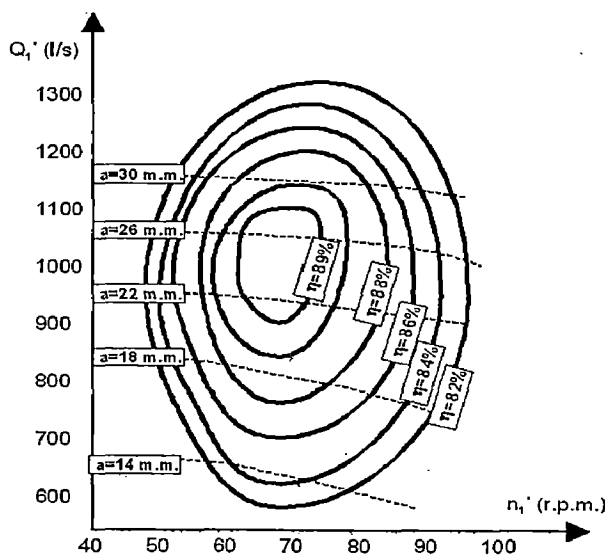$$Q = Q_1 D_1^2 \sqrt{H} \qquad\qquad (2.1)$$

Fig. 2.1   Efficiency hill curve of a Francis Turbine

16

However, if it were possible to modify the speed, n, the efficiency could be optimized for given operating conditions. Moreover, the speed adjustment would avoid other problems that arise when the head deviations are excessive, namely draft tube pressure oscillations and cavitations [13], [14], and [15].

2.2 Propeller and Kaplan Turbines

The double regulation of a Kaplan turbine allows maintaining high values of efficiency in a broad range of values of head and discharge. A propeller turbine has fixed blades; its cost being appreciably lower than that of a Kaplan turbine [1]. However, the efficiency drops dramatically for load values out of a narrow range in the neighborhood of rated power. As before, variable-speed operation of a propeller turbine substantially improves its performance, although keeping it below that of a Kaplan turbine. Moreover, in some power plant configurations it would be possible to operate without wicket gates, where regulation is provided by the speed. Thus , the variable-speed propeller turbine may be a good alternative to a Kaplan turbine because of its greater simplicity and robustness, with maintaining good performance. The counterpart comes from the extra equipment needed for variable-speed operation on a fixed-frequency grid.

2.3 The basic idea of variable speed operation

The idea of VSO of a turbine is to allow the turbine speed to change with hydraulic conditions in order to maximize the turbine efficiency. Figure 2.2 A shows the velocity vectors at the turbine blades at design flow. For a lower flow (Figure 2.1 B), the guide vanes are closed and the turbine blades are turned accordingly. In case of the variable speed propeller turbine (Figure 2.2 C), the speed is reduced in proportion with flow in such a way, that the fluid velocity vectors match the design conditions.

17
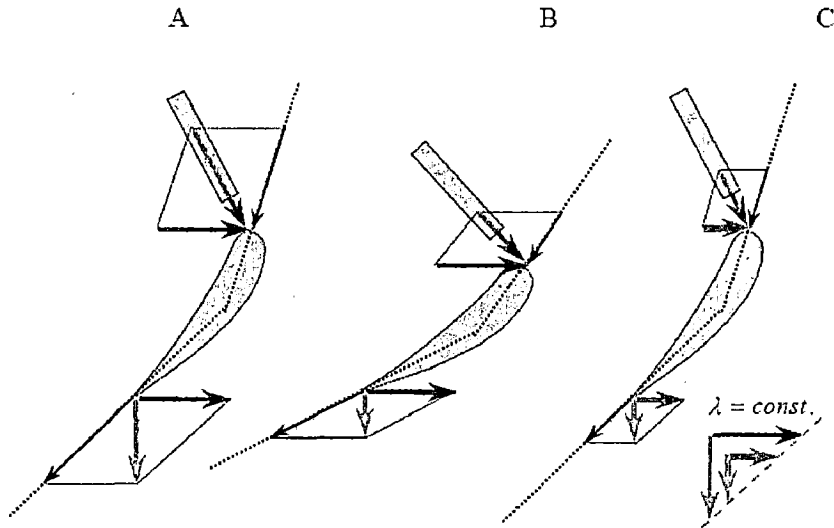
Figure 2.2: Fluid velocity vectors at design condition and for a low flow [3]

The realistic behavior of turbine operating at variable speed is shown in the hill charts which are normally determined from model tests. Today, double regulated Kaplan turbines are designed for a fixed speed and so, the maximum efficiency does not vary with speed, as shown in Figure 2.3 - A. The same turbine operating as propeller turbine shows a very narrow area of high efficiency around the Q~n line. The typical efficiency curve of such a propeller turbine is shown in Figure 2.3 B. Operating at variable speed, the efficiency follows the Q~n line and so, we find a high efficiency over a wide operating range.
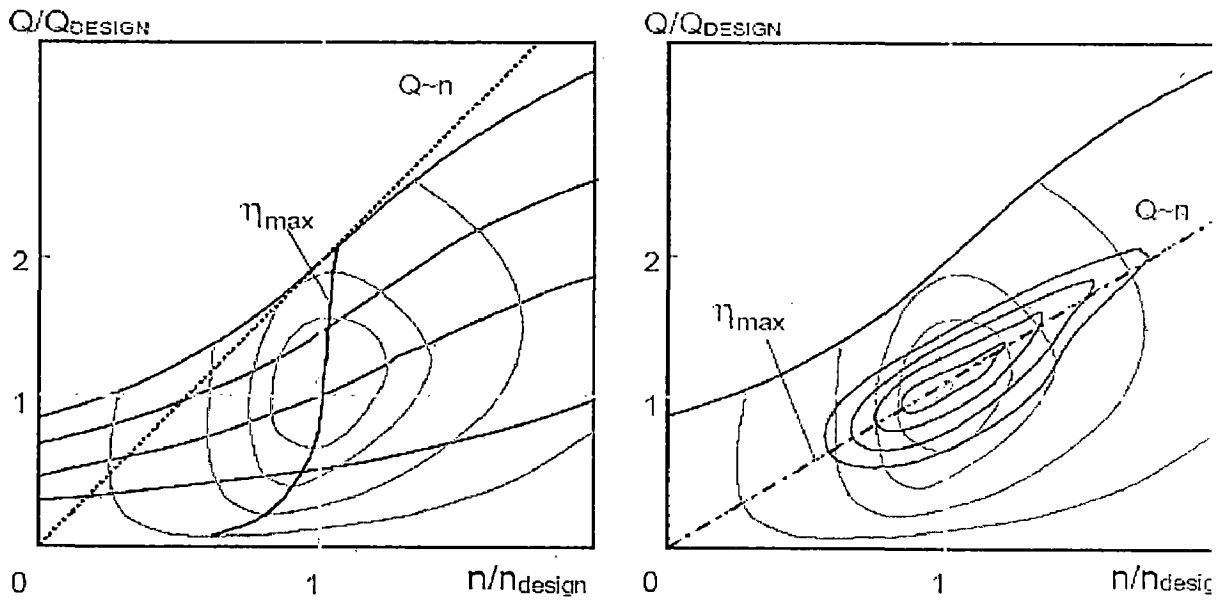
Figure 2.3: Idealized hill charts of A: Kaplan (left) and B: propeller turbine (right)Bard

2.4 Simulation of Hydro Turbine

The relationship between the net head and discharge has to be specified to a turbine in a hydraulic transient model. Flow through a turbine depends on various parameters for example , the flow through Francis turbine depends on the net head, rotational speed of the unit, and wicket gate opening, while the flow through Kaplan turbine depends on the same variable as defined above as well as runner blade angle . Curve representing these parameters are called turbine characteristics.

Typical characteristic of a Francis turbine is shown in Fig 2.4 . In these figures the abscissa is the unit speed, φ , and the ordinates are the unit flow, q, and the unit power ,p. Where D= diameter of runner ,N= rotational speed, Hn= net head, Q= turbine discharge; and P = power output .
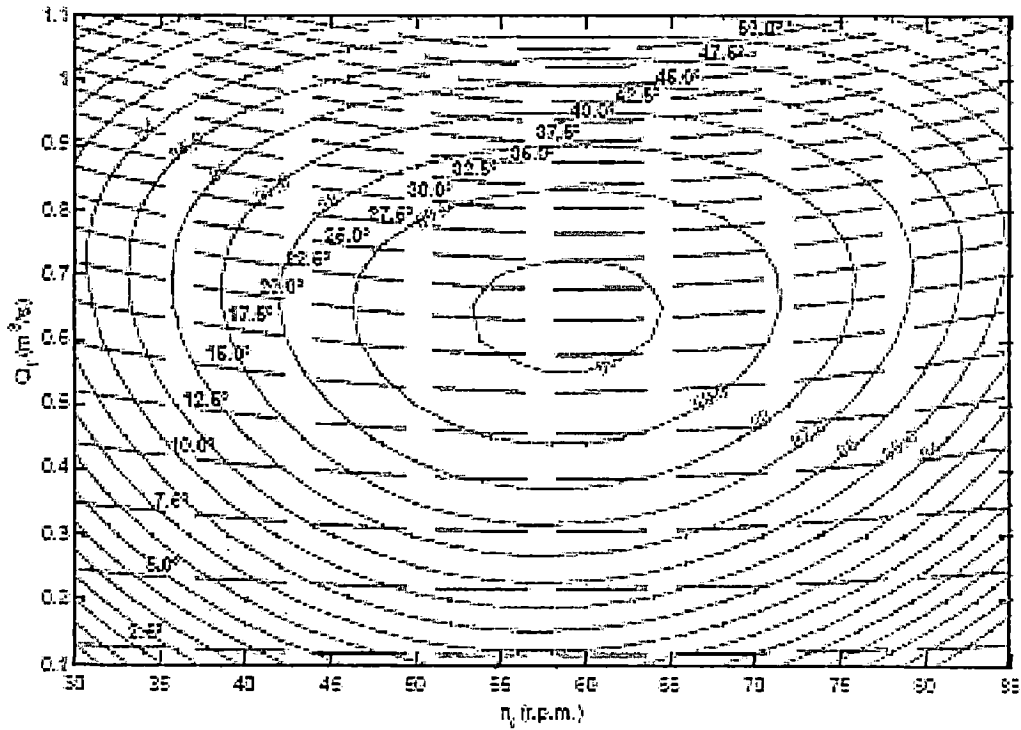
Fig. 2.4 Hill Curve for Francis Turbine

A grid of point on the characteristic curve for the various gate openings are stored in computer, and unit discharge, an unit power at intermediate gate opening and φ values are determined by parabolic interpolation .

The boundary conditions for a turbines are derived below. Referring to 2.4

$$H_p = H_n = H_{tail} - \frac{Q_P^2}{2gA^2}$$ (2.3).

Where H_p = instantaneous piezometric head at the entrance; H_n =instantaneous net head; H_{tail} = tail water level above datum; Q_p = instantaneous flow at the entrance to the scroll case ; and A = cross-sectional area of the pressure conduit at the turbine inlet. H_p, Q_P and H_n are values of these variables at the end of time step under consideration. Let the wicket gate opening at the end of time step be τ_P .

20

Reservoir

Hydraulic Grade line

$$\frac{Q^2_P}{2_g A^2}$$

Hn

Hp

Penstock

Turbine

tail race

Qp

H tail

Datum line
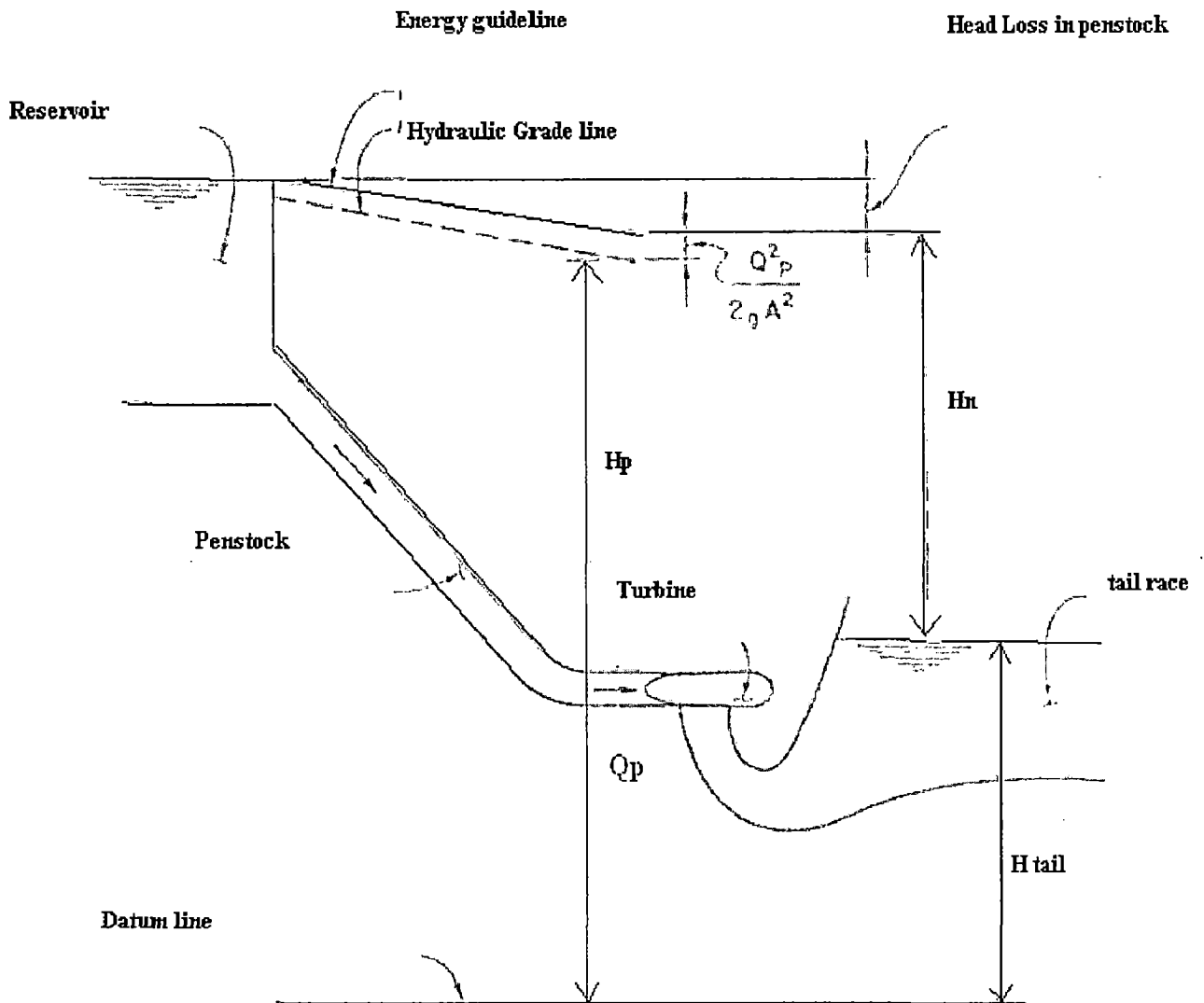
Fig.2.4 Notation for boundary condition for a Francis turbine

The value of four variables, namely H_P, τ_P, Q_P and N_P are unknown at end of time step under consideration. and may be determined by the iterative procedure. Because the transient- state turbine speed and gate opening vary gradually, above parameter can be estimated as a first approximation by parabolic extrapolation.
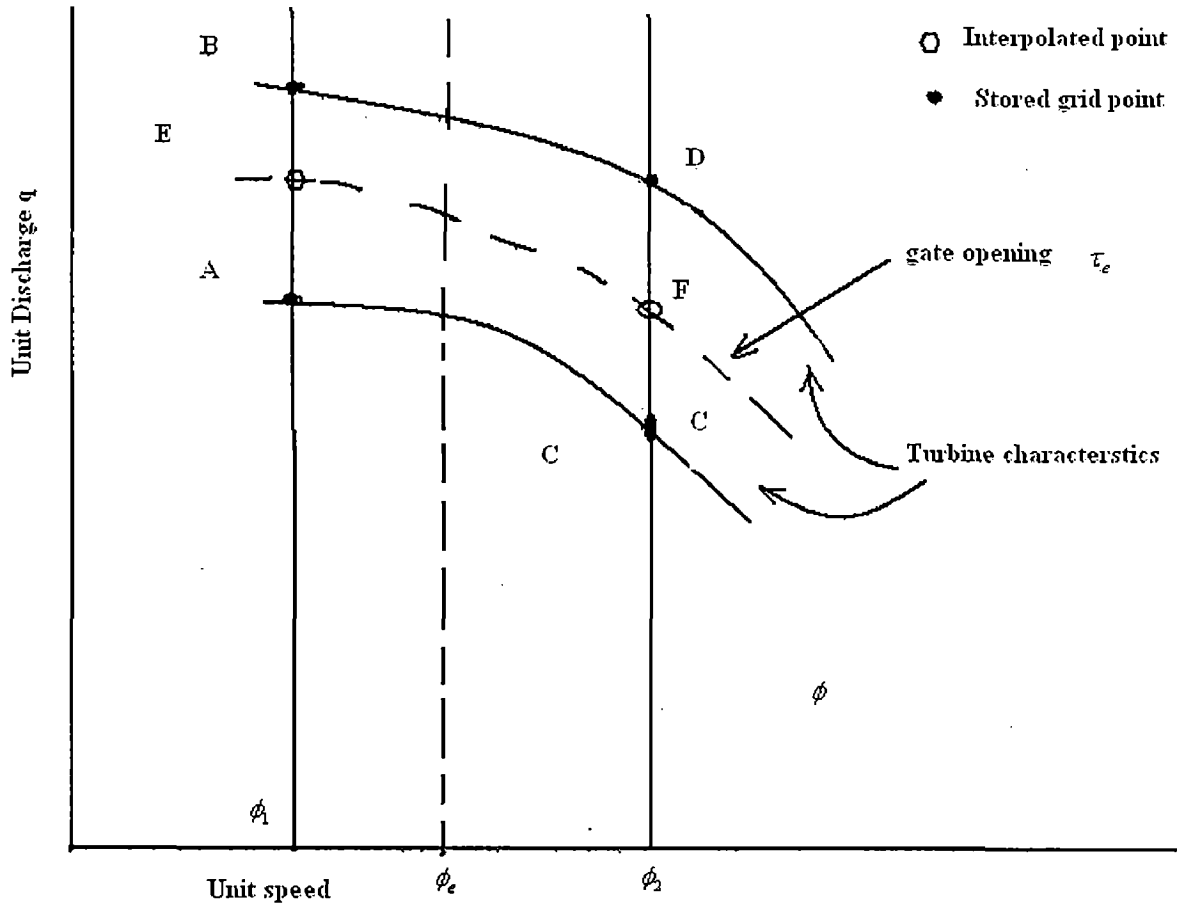
Fig. Interpolation of turbine characteristics

Let the value of τ_p H_n and N_p estimated by extrapolation be τ_e H_{ne} and N_e and unit speed is φ_e. The characteristic for τ_e for φ between φ_1 and φ_2 may be approximated by the straight line EF. As shown in figure *4.3* the value at E are interpolated from the known values at points C & D.

The equation of straight line EF may be written as

$$q = a_0 + a_1 \phi \qquad (2.4)$$

In which a_0 and a_1 are determined from the known coordinates of E &F.

22

Substituting q and ϕ from equation (4.1) and (4.2) (SI unit)

$$a_2\sqrt{H_n} = Q_P - a_3 \qquad\qquad (2.5)$$

In which,

$$a_2 = a_0 D^2$$
and $\qquad\qquad\qquad\qquad\qquad (2.6)$
$$a_3 = N_e D^3 \, a_1 / 84.45$$

Combining equation (2.3) and general equation $Q_P = C_P - C_a H_P$;

$$Q_P = (C_P - C_a H_{tail}) + \frac{C_a Q^2{}_P}{2gA^2} - C_a H_n \qquad\qquad (2.7)$$

where $\quad C_P = Q_A + \dfrac{gA}{a} H_A - \dfrac{f\Delta t}{2DA} Q_A |Q_A|$

         f = Darcy-Weisbach friction factor)

         g = gravitational constant

         A = cross sectional area of the conduit

         D = diameter of the conduit

         f = Darcy-Weisbach friction factor

         c = celerity of a compression wave traveling
                through the penstock

Squaring (2.5) ,eliminating H_n from the resulting equation and Eq. (2.7), we get

$$a_4 Q_P^2 + a_5 \, Q_P + a_6 = 0 \qquad\qquad (2.8)$$

where

$$a_4 = \frac{c_a}{2A^2 g} - \frac{C_a}{a_2^2}$$

$$, a_5 = \frac{2a_3 C_a}{a_2^2} - 1$$

$$a_6 = C_p - C_a H_{tail} - \frac{C_a a_3^2}{a_2^2}$$

Solution of equation (4.8) yields

$$Q_P = \frac{-a_5 - \sqrt{a_5^2 - 4a_4 a_6}}{2a_4} \qquad (2.9)$$

Because of instantaneous unbalanced torque , $T_u = T_{tur} - T_{gen}$,the speed of turbine and generator set changes according to equation

$$T_u = WR^2 \frac{d\omega}{dt}$$

or   (2.10)

$$T_{tur} - T_{gen} = WR^2 \frac{2\pi}{60} \frac{dN}{dt}$$

$\eta_{gen} = $ generator efficiency , $T_{tur} = $ instantaneous turbine torque $T_{gen} = $ instantaneous

generator torque . ω, rotational speed of turbine generator, $WR^2 = $ total moment of

inertia of the turbine and generator in kg m^2 .

$$P_{tur} - \frac{P_{gen}}{\eta_{gen}} = WR^2 (\frac{2\pi}{60})^2 N \frac{dN}{dt} \qquad (2.11)$$

in which $P_{gen} = $ generated load ,and $P_{tur} = $ power devlopped by the turbine.

Integrating both side we have

$$\int_{t1}^{tp}(P_{tur} - \frac{P_{gen}}{\eta_{gen}})dt = 1.097 \times 10^{-2} WR^2 \int_{N1}^{Np} NdN$$

simplifying (2.12)

$$\left(\frac{P_{tur1} + P_{turP}}{2} - \frac{P_{gen1} + P_{genP}}{2\eta_{gen}} \right) \Delta t = 0.548 \times 10^{-12} WR^2 (N_P^2 - N_1^2)$$

In which subscript 1 and P indicate the values of the variables at the beginning and at the end of time step . solving for N_p,

$$N_P = \left\{ N_1^2 + 182.38 \frac{\Delta t}{WR^2} \left[0.5(P_{tur1} + P_{turP}) - \frac{0.5}{\eta_{gen}}(P_{gen1} + P_{genP}) \right] \right\}^{0.5}$$ (2.13)

2.5 Hydraulic Turbine Governors

Governors are provided to keep the turbo generator speed at desired level. The main components of the governor are speed sensing device and a servomechanism for opening and closing the wicket gates.

Three types of governors are used for the hydro turbines:

(1) Dashpot

(2) Accelerometric

(3) Proportional –integral –derivative (PID)

In dashpot governors, the corrective action of the governor is proportional to the speed deviation, n; in the accelerometric governor, it is proportional to dn/dt. In the PID, it is proportional to n, dn/dt, and time integral of n. In this work dashpot governor is discussed.

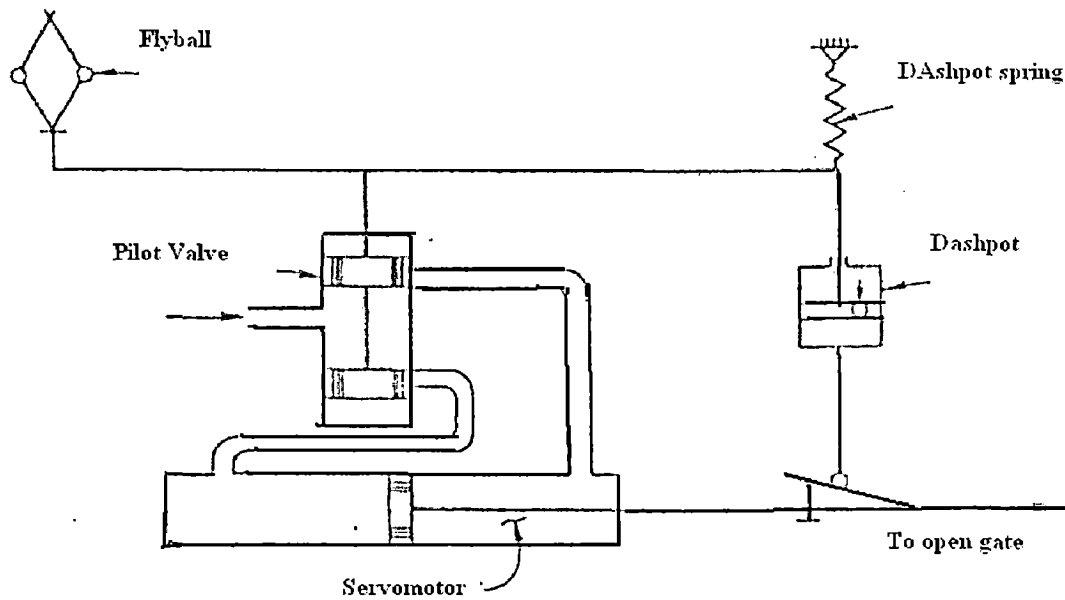Dashpot governor scheme is shown in figure 2.5 .

Fig.2.6 Dashpot Governor

Following a load increase (decrease), sequence of events is as follows:

The speed of unit decrease (increase) because of load change, and the fly ball move inward (outward). This displaces the piston of pilot valve, and the oil is admitted in to the hydraulic servo that opens (close) the wicket gates. As a result of the wicket gate movement the dashpot spring is compressed, which change the position of pilot valve. After some time the dashpot spring returns to its original position because of oil flow through the small orifice in the dashpot, even though the servo and the wicket gates are now at a different position.

T_a = actuator time constant

T_r =Dashpot time constant

σ = permanent speed droop

δ = temporary speed droop

26

T_d = distributing valve time constant

k_d = distributing valve gain

k_s = gate servomotor gain

n   = normalized transient- state turbine speed

The synchronous speed of the turbo generator set , N_R is used to normalized the turbine

speed , i.e. n= N/N_R. If τ_o be the initial steady state wicket gate opening, then

$$n_{ref} = 1 + \sigma\tau_0 .$$

Actuator

$$v_a = \frac{1}{T_a s} e$$

$$e = T_a \frac{dv_a}{dt} \qquad\qquad 0 \le v_a \le 1 \qquad\qquad\qquad (2.14)$$

Dashpot

$$e_t = \frac{\delta T_r s}{1 + T_s s} v_a$$

or $\qquad\qquad e_t + T\ r\ \dfrac{de_t}{dt} - \delta T_r \dfrac{dv_a}{dt} = 0 \qquad -e_{t\max} \le e_t \le e_{t\max} \qquad (2.15)$

Permanent Drop

$$e_d - \sigma v_a = 0$$

Distributing valve

$$v_a = \frac{k_d}{1 + T_d s} v_i$$

$$T_d \frac{dv_d}{dt} + v_d - k_d v_i = 0$$

$$T_d \frac{dv_d}{dt} + v_d - k_d v_i = 0 \qquad\qquad v_{d\,min} \leq v_d \leq v_{d\,max} \qquad\qquad (2.16)$$

$$\tau = \frac{k_s}{s} v_d$$

Gate Servomotor *thus* $\qquad\qquad\qquad\qquad\qquad 0 \leq \tau \leq 1 \qquad\qquad (2.17)$

$$\frac{d\tau}{dt} - k_s v_d = 0$$

The following equations may be written because of two feedbacks

$$e = n_{ref} - e_d - e_t - n$$

and

$$v_i = v_a - \tau$$

Output of various components may saturate and that these saturation limits must be taken in to consideration in analysis of large load changes.

By eliminating e ,e_d and v_i and rearranging above equations we get

$$\frac{dv_a}{dt} = \frac{1}{Ta}(n_{ref} - n - e_t - \sigma v_a) \qquad\qquad (2.17)$$

$$\frac{de_t}{dt} = \frac{1}{T_r}(\delta T_r \frac{dv_a}{dt} - e_t) \qquad\qquad (2.18)$$

$$\frac{dv_d}{dt} = \frac{1}{T_d}[k_d(v_a - \tau) - v_d] \qquad\qquad (2.19)$$

$$\frac{d\tau}{dt} = k_s v_d \qquad\qquad (2.20)$$

The preceding four differential equations in four variables, namely ,v_a,e_t,v_d and τ may be integrated by any standard numerical technique; a close form of solution is not possible because of nonlinearities introduced by the saturation of various variables.
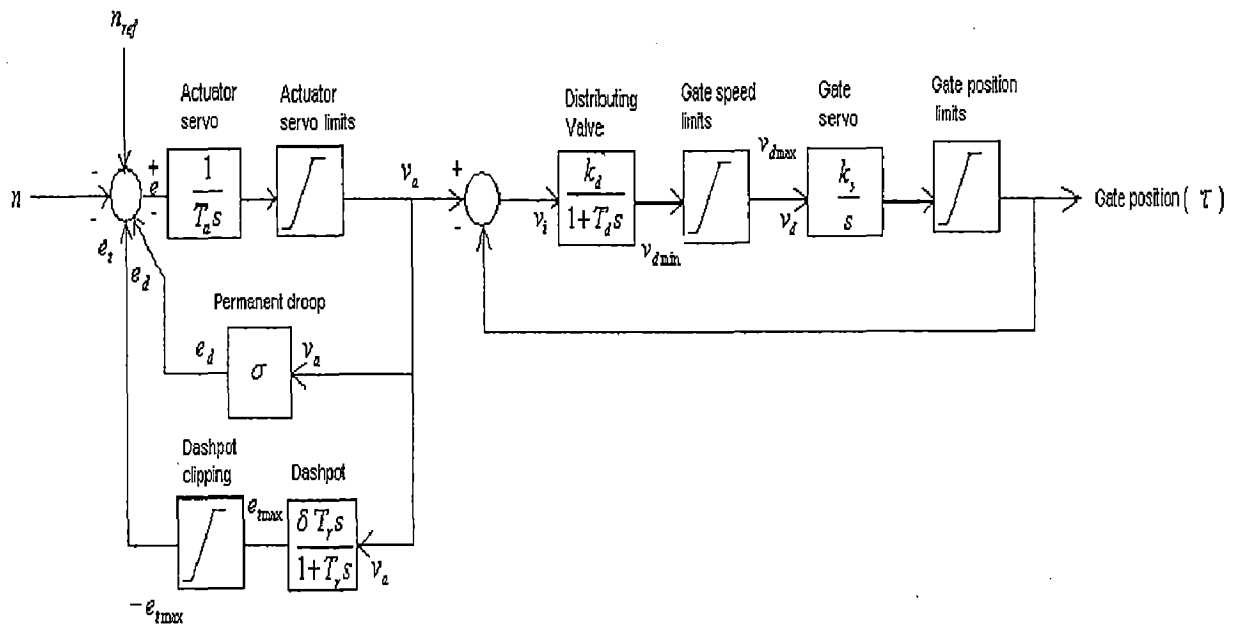
28

Fig. 2.7 Block diagram for Dashpot Governor

MATHEMATICAL MODEL OF THE INDUCTION GENERATOR

3.1 Basic equations of the induction machine model

3.1.1 Voltage equations

The stator voltage equations for induction generator are given by

$$v_{ks} = \frac{d\lambda_{ks}}{dt} + r_s i_{ks} \qquad \text{k= a, b, c} \tag{3.1}$$

Rotor Voltage equation is given by

$$v_{kr} = \frac{d\lambda_{kr}}{dt} + r_r i_{kr} \qquad \text{k= a, b, c} \tag{3.2}$$

where, subscript s and r are expressed quantities of Stator and rotor $\lambda_{kr}, \lambda_{ks}$ are the flux linkages; r_s, r_s are winding resistances.

3.1.2 Flux linkage equations

In matrix notation, the flux linkages of the stator and rotor windings, in terms of the winding inductances and currents, can be written as

$$\begin{bmatrix} \lambda_s^{abc} \\ \lambda_r^{abc} \end{bmatrix} = \begin{bmatrix} L_{ss}^{abc} & L_{sr}^{abc} \\ L_{rs}^{abc} & L_{rr}^{abc} \end{bmatrix} \begin{bmatrix} i_s^{abc} \\ i_r^{abc} \end{bmatrix} \tag{3.3}$$

where

$$\lambda_s^{abc} = (\lambda_{as}, \lambda_{bs}, \lambda_{cs}), \qquad \lambda_r^{abc} = (\lambda_{ar}, \lambda_{br}, \lambda_{cr})'$$

$$i_s^{abc} = (i_{as}, i_{bs}, i_{cs})' \qquad i_r^{abc} = (i_{ar}, i_{br}, i_{cr})'$$

and the subscript t denotes the transpose of the array. The sub matrices of the stator-to-stator and rotor-to-rotor winding inductances are in the form:

$$L_{ss}^{abc} = \begin{bmatrix} L_{ls}+L_{ss} & L_{sm} & L_{sm} \\ L_{sm} & L_{ls}+L_{ss} & L_{sm} \\ L_{sm} & L_{sm} & L_{ls}+L_{ss} \end{bmatrix}$$

(3.4)

$$L_{rr}^{abc} = \begin{bmatrix} L_{lr}+L_{rr} & L_{rm} & L_{rm} \\ L_{rm} & L_{lr}+L_{rr} & L_{rm} \\ L_{rm} & L_{rm} & L_{lr}+L_{rr} \end{bmatrix}$$

(3.5)

where L_{ls} is the per phase stator winding leakage inductance L_{lr} the per phase rotor winding leakage inductance, L_{ss} the self-inductance of the stator winding, L_{rr} the self-inductance of the rotor winding, L_{sm} the mutual inductance between stator windings and L_{rm} the mutual inductance between rotor windings.

The stator-to-rotor mutual inductances are dependent on the rotor angle, described by the following matrix

$$L_{sr}^{abc} = \left[L_{rs}^{abc} \right]^t$$

31

$$= L_{sr} \begin{bmatrix} \cos\theta_r & \cos(\theta_r + \frac{2}{3}\pi) & \cos(\theta_r - \frac{2}{3}\pi) \\ \cos(\theta_r - \frac{2}{3}\pi) & \cos\theta_r & \cos(\theta_r + \frac{2}{3}\pi) \\ \cos(\theta_r + \frac{2}{3}\pi) & \cos(\theta_r - \frac{2}{3}) & \cos\theta_r \end{bmatrix} \qquad (3.6)$$

where L_{sr} is the peak value of the stator-to-rotor mutual inductance.

3.1.3 Transformation:

The transformation equation from abc to $qd0$ reference frame is given by

$$\begin{bmatrix} f_q \\ f_d \\ f_0 \end{bmatrix} = [T_{qd0}(\theta)] \begin{bmatrix} f_a \\ f_b \\ f_c \end{bmatrix} \qquad (3.7)$$

where the variable f can be the phase voltage, current, or flux linkage of the machine, the

$qd0$ transformation matrix, $[T_{qd0}(\theta)]$

$$[T_{qd0}(\theta)] = \frac{2}{3} \begin{bmatrix} \cos\theta & \cos(\theta - \frac{2}{3}\pi) & \cos(\theta + \frac{2}{3}\pi) \\ \cos(\theta) & \cos(\theta - \frac{2}{3}\pi) & \sin(\theta + \frac{2}{3}\pi) \\ \frac{1}{2} & \frac{1}{2} & \frac{1}{2} \end{bmatrix} \qquad (3.8)$$

dq0 voltage equations in matrix notation stator winding a b c voltage equation can be expressed as

$$V_s^{abc} = p \lambda_s^{abc} + r_s^{abc} i_s^{abc} \qquad (3.9)$$

Applying the transformation $[T_{qd0}(\theta)]$ to the voltage flux linkage and current

Equation (9) becomes

32

$$v_s^{qd0} = \omega \begin{bmatrix} 0 & 1 & 0 \\ -1 & 0 & 0 \\ 0 & 0 & 0 \end{bmatrix} \lambda_s^{qd0} + p\lambda_s^{qd0} + r_s^{dq0} i_s^{dqo} \tag{3.10}$$

where

$$\omega = \frac{d\theta}{dt}, r_s = \begin{bmatrix} 1 & 0 & 0 \\ 0 & 1 & 0 \\ 0 & 0 & 0 \end{bmatrix}$$

Using the transformation, $\left[T_{qd0}(\theta)\right]$, to the rotor voltage equations, in the same manner as we have done with the stator voltage equations. The following $qd0$ voltage equation for the rotor windings:

$$v_r^{dq0} = (\omega - \omega_r)\begin{bmatrix} 0 & 1 & 0 \\ -1 & 0 & 0 \\ 0 & 0 & 0 \end{bmatrix}\lambda_r^{qd0} + p\lambda_r^{dq0} + r_r^{dq0} i_r^{dq0} \tag{3.11}$$

qd0 flux linkage equations:

The stator $qd0$ flux linkage are obtained by applying $\left[T_{dq0}(\theta)\right]$ to the stator abc flux linkages in Equation (3),

$$\lambda_s^{dq0} = \left[T_{qd0}^{abc}(\theta)\right]\left[L_{ss}^{abc} i_s^{abc} + L_{sr}^{abc} i_r^{abc}\right]$$

$$= \begin{bmatrix} L_{ls} + \frac{3}{2}Lss & 0 & 0 \\ 0 & L_{ls} + \frac{3}{2}L_{ss} & 0 \\ 0 & 0 & L_{ls} \end{bmatrix} i_s^{qd0} + \begin{bmatrix} \frac{3}{2}L_{sr} & 0 & 0 \\ 0 & \frac{3}{2}L_{sr} & 0 \\ 0 & 0 & 0 \end{bmatrix} i_r^{qd0} \tag{3.12}$$

Similarly, the *qd0* rotor flux linkages are given by

$$
\lambda_r^{qd0} = \begin{bmatrix} L_{lr} + \dfrac{3}{2}L_{rr} & 0 & 0 \\ 0 & L_{lr} + \dfrac{3}{2}L_{rr} & 0 \\ 0 & 0 & L_{lr} \end{bmatrix} i_r^{qd0} + \begin{bmatrix} \dfrac{3}{2}L_{sr} & 0 & 0 \\ 0 & \dfrac{3}{2}L_{sr} & 0 \\ 0 & 0 & 0 \end{bmatrix} i_s^{qd0}
$$

(3.13)

The stator and rotor flux linkage relationships in Equations (12) and (13) can be expressed as

$$
\lambda_{qs} = L_{ls}i_{qs} + L_m(i_{qs} + i'_{qr})
$$

(3.14)

$$
\lambda_{ds} = L_{ls}i_{ds} + L_m(i_{ds} + i'_{dr})
$$

(3.15)

$$
\lambda_{0s} = L_{ls}i_{0s}
$$

(3.16)

$$
\lambda'_{qr} = L'_{lr}i'_{qr} + L_m(i_{qs} + i'_{qr})
$$

(3.17)

$$
\lambda'_{dr} = L'_{lr}i'_{dr} + L_m(i_{ds} + i'_{dr})
$$

(3.18)

$$
\lambda'_{0r} = L'_{lr}i'_{0r}
$$

(3.19)

where the prime rotor quantities denote reffered valued to the stator side according to the following relationship

$$
\lambda'_{qr} = \frac{N_s}{N_r}\lambda_{qr}, \quad \lambda'_{dr} = \frac{N_s}{N_r}\lambda_{dr},
$$

$$i'_{qr} = \frac{N_r}{N_s} i_{qr}, \qquad i'_{dr} = \frac{N_r}{N_s} i_{dr},$$

$$L'_{lr} = \left(\frac{N_s}{N_r}\right)^2 L_{lr} \tag{3.20}$$

and L_m the magnetizing inductance on the stator side is

$$L_m = \frac{3}{2} L_{ss} = \frac{3}{2} \frac{N_s}{N_r} L_{sr} = \frac{3}{2} \frac{N_s}{N_r} L_{rr} \tag{3.21}$$

where Ns is the stator winding turns, N_r, is rotor winding turns.

3.1.4 Torque equations

The sum of the instantaneous input power to all six windings of the stator and rotor is given by

$$P_{in} = v_{as} i_{as} + v_{bs} i_{bs} + v_{cs} i_{cs} + v'_{ar} i'_{ar} + v'_{br} i'_{br} + v'_{cr} i'_{cr} \tag{3.22}$$

In terms of the $qd0$ quantities, the instantaneous input power is

$$P_{in} = \frac{3}{2} (v_{qs} i_{qs} + v_{ds} i_{ds} + 2 v_{0s} i_{0s} + v'_{qr} i'_{qr} + v'_{br} i'_{dr} + 2 v'_{0r} i'_{0r} \tag{3.23}$$

The electromechanical torque developed by the sum of the $\omega \lambda i$ terms of the equation which substituted Equations (10) and (11) in Equation (23) divided by mechanical speed, that is,

$$T_{em} = \frac{3}{2} \frac{P}{2\omega_r} \left[\omega (\lambda_{ds} i_{qs} - \lambda_{qs} i_{ds}) + (\omega - \omega_r)(\lambda'_{dr} i'_{qr} - \lambda'_{qr} i'_{dr}) \right] \tag{3.24}$$

Using the flux linkage relationship in Equations (17) and (18), equation (24) can be expressed in the following form:

35

$$T_{em} = \frac{3}{2}\frac{P}{2}\left[L_m\left(i'_{dr}\,i_{qs} - i'_{qr}\,i_{ds}\right)\right]$$

<div align="right">(3.25)</div>

qd0 stationary reference frame

The induction machine equations in stationary reference frame can be obtained from generalized equations by simply substituting w=0. The stator and rotor voltage equations are given by

Stator voltage equations

$$v_{ls} = \frac{d\lambda_{ls}}{dt} + r_s i_{ls} \qquad\qquad l = d,q,0$$

<div align="right">(3.26)</div>

Rotor voltage equations

$$v'_{qr} = \frac{d\lambda'_{qr}}{dt} - \omega_r \lambda'_{dr} + r'_r i'_{qr}$$

<div align="right">(3.27)</div>

$$v'_{dr} = \frac{d\lambda'_{dr}}{dt} + \omega_r \lambda'_{qr} + r'_r i'_{dr}$$

<div align="right">(3.28)</div>

$$v'_{0r} = \frac{d\lambda'_{0r}}{dt} + r'_r i'_{0r}$$

<div align="right">(3.29)</div>

The flux linkage equation and torque can be given by

Flux linkage equation

$$\lambda_{qs} = L_{ls} i_{qs} + L_m\left(i_{qs} + i'_{qr}\right)$$

<div align="right">(3.30)</div>

$$\lambda_{ds} = L_{ls} i_{ds} + L_m\left(i_{ds} + i'_{dr}\right)$$

<div align="right">(3.31)</div>

$$\lambda_{0s} = L_{ls} i_{0s}$$

<div align="right">(3.32)</div>

$$\lambda'_{qr} = L'_{lr} i'_{qr} + L_m\left(i_{qs} + i'_{qr}\right)$$

<div align="right">(3.33)</div>

$$\lambda'_{dr} = L'_{lr} i'_{dr} + L_m (i_{ds} + i'_{dr})$$

(3.34)

$$\lambda'_{0r} = L'_{lr} i'_{0r}$$

(3.35)

Equation of motion of rotor

Torque equation

$$T_{em} = \frac{3}{2} \frac{P}{2} \left[L_m (i'_{dr} i_{qs} - i'_{qr} i_{ds}) \right]$$

(3.36)

Equation of motion of the rotor

The equation of motion of the rotor is obtained by equating the inertia torque to the

accelerating torque

$$j \frac{d\omega_{rm}}{dt} = T_{em} + T_{mech} - T_{damp}$$

(3.37)

where T_{mech} is the externally-applied mechanical torque T_{damp} is the damping torque.

3.2 Computer Simulation in the Synchronous Reference frame.

Generally machine equations are expressed in term of the flux linkage per seconds, ψ''s

and reactance, x' s instead of λ ' s and L's .These are related by the base value of angular

frequency , wb, that is

$$\psi = \omega_b \lambda \qquad \text{V or per unit}$$

(3.38)

$$x = \omega_b L \qquad \Omega$$

(3.39)

Now equation for the simulation of induction machine will be given as below[10]

$$i_{qs} = \frac{1}{x_{ls}} (\psi_{qs} - \psi_{mq})$$

(3.40)

$$i_{ds} = \frac{1}{x_{ls}}\left(\psi_{ds} - \psi_{md}\right)$$

(3.41)

$$i_{0s} = \frac{1}{x_{ls}}\left(\psi_{0s}\right)$$

(3.42)

$$i'_{qr} = \frac{1}{x'_{lr}}\left(\psi'_{qr} - \psi_{mq}\right)$$

(3.43)

$$i'_{dr} = \frac{1}{x'_{lr}}\left(\psi'_{dr} - \psi_{md}\right)$$

(3.44)

$$i'_{0r} = \frac{1}{x'_{lr}}\left(\psi'_{0r}\right)$$

(3.45)

$$\psi_{mq} = X_M\left(i_{qs} + i'_{qr}\right)$$

(3.46)

$$\psi_{md} = X_M\left(i_{ds} + i'_{dr}\right)$$

(3.47)

If (3.40) - (3.45) are used to eliminate the current in (3.46) and (3.47) as well as in voltage equations ,then flux linkages per second may be written in following integral equation form :

$$\psi_{qs} = \frac{w_b}{p}\left[v_{qs} - \frac{w_e}{w_b}\psi_{ds} + \frac{r_s}{x_{ls}}\left(\psi_{mq} - \psi_{qs}\right)\right]$$

(3.48)

$$\psi_{ds} = \frac{w_b}{p}\left[v_{ds} - \frac{w_e}{w_b}\psi_{qs} + \frac{r_s}{x_{ls}}\left(\psi_{md} - \psi_{ds}\right)\right]$$

(3.49)

$$\psi_{0s} = \frac{w_b}{p}\left[v_{0s} - \frac{r_s}{x_{ls}}\left(\psi_{md} - \psi_{0s}\right)\right]$$

(3.50)

$$\psi'_{qr} = \frac{w_b}{p}\left[v'_{qr} - \frac{(w_e - w_r)}{w_b}\psi'_{dr} + \frac{r'_r}{x'_{lr}}\left(\psi_{mq} - \psi'_{qr}\right)\right]$$

(3.51)

38

$$\psi'_{dr} = \frac{w_b}{p}\left[v'_{dr} + \frac{(w_e - w_r)}{w_b}\psi'_{qr} + \frac{r'_r}{x'_{lr}}(\psi_{md} - \psi'_{dr})\right] \qquad (3.52)$$

$$\psi'_{0r} = \frac{w_b}{p}\left[v'_{0r} - \frac{r'_r}{x'_{lr}}(\psi'_{0r})\right] \qquad 3.53)$$

$$\psi_{mq} = X_{aq}\left(\frac{\psi_{qs}}{x_{ls}} + \frac{\psi'_{qr}}{x'_{lr}}\right) \qquad (3.54)$$

$$\psi_{md} = X_{ad}\left(\frac{\psi_{ds}}{x_{ls}} + \frac{\psi'_{dr}}{x'_{lr}}\right) \qquad (3.55)$$

In which

$$X_{aq} = x_{ad} = \left(\frac{1}{X_M} + \frac{1}{X_{ls}} + \frac{1}{X'_{lr}}\right)^{-1} \qquad (3.56)$$

$$Te = \psi_{ds}i_{qs} - \psi_{qs}i_{ds} \quad \text{pu} \qquad (3.57)$$

$$\frac{1}{2H}\frac{d\omega_{rm}}{dt} = T_{em} + T_{mech} - T_{damp}$$

CONTROL OF DOUBLY FED INDUCTION GENERATOR

The hydro turbine and the doubly-fed induction generator are shown in the figure called "The Hydro turbine and the doubly-fed induction generator system" in fig. 4.1. MATLAB diagram of the DFIG with its control blocks is shown in figure 4.2. The AC/DC/AC converter is divided into two components: the rotor-side converter (Crotor) and the grid-side converter (Cgrid). Crotor and Cgrid are Voltage-Sourced Converters that use forced-commutated power electronic devices (IGBTs) to synthesize an AC voltage from a DC voltage source. A capacitor connected on the DC side acts as the DC voltage source. A coupling inductor L is used to connect Cgrid to the grid. The three-phase rotor winding is connected to Crotor by slip rings and brushes and the three-phase stator winding is directly connected to the grid. The power captured by the Hydro turbine is converted into electrical power by the induction generator and it is transmitted to the grid by the stator and the rotor windings. The control system generates the voltage command signals V_r and V_{gc} for Crotor and Cgrid respectively in order to control the power of the Hydro turbine, the DC bus voltage and the reactive power or the voltage at the grid terminals.

Terms used in figure are described below:

P_m Mechanical power captured by the Hydro turbine and transmitted

     to the rotor

P_s Stator electrical power output
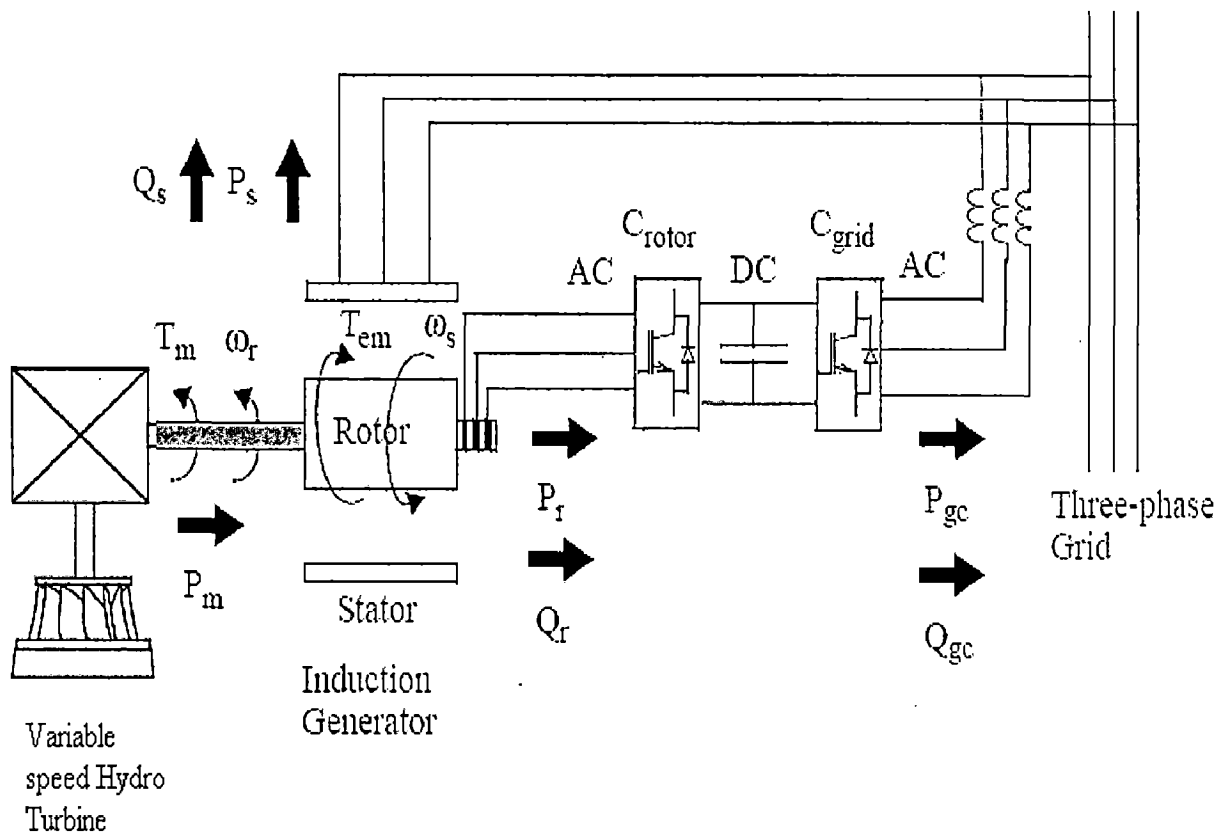
Fig. 4.1 Hydro Turbine with DFIG (Power Flow)

P_r Rotor electrical power output

P_{gc} Cgrid electrical power output

Q_s Stator reactive power output

Q_r Rotor reactive power output

Q_{gc} Cgrid reactive power output

T_m Mechanical torque applied to rotor

T_{em} Electromagnetic torque applied to the rotor by the generator

ω_r Rotational speed of rotor

ω_s Synchronous Sped

J Combined rotor and Hydro turbine inertia coefficient

4.1 The Power Flow

Generally the absolute value of slip is much lower than one and, consequently, P_r is only a fraction of P_s. Since T_m is positive for power generation and since ω_s is positive and constant for a constant frequency grid voltage, the sign of P_r is a function of the slip sign. P_r is positive for negative slip (speed greater than synchronous speed) and it is negative for positive slip (speed lower than synchronous speed). For super-synchronous speed operation, P_r is transmitted to DC bus capacitor and tends to rise the DC voltage. For sub-synchronous speed operation, P_r is taken out of DC bus capacitor and tends to decrease the DC voltage. Cgrid is used to generate or absorb the power P_{gc} in order to keep the DC voltage constant. In steady-state for a loss less AC/DC/AC converter P_{gc}
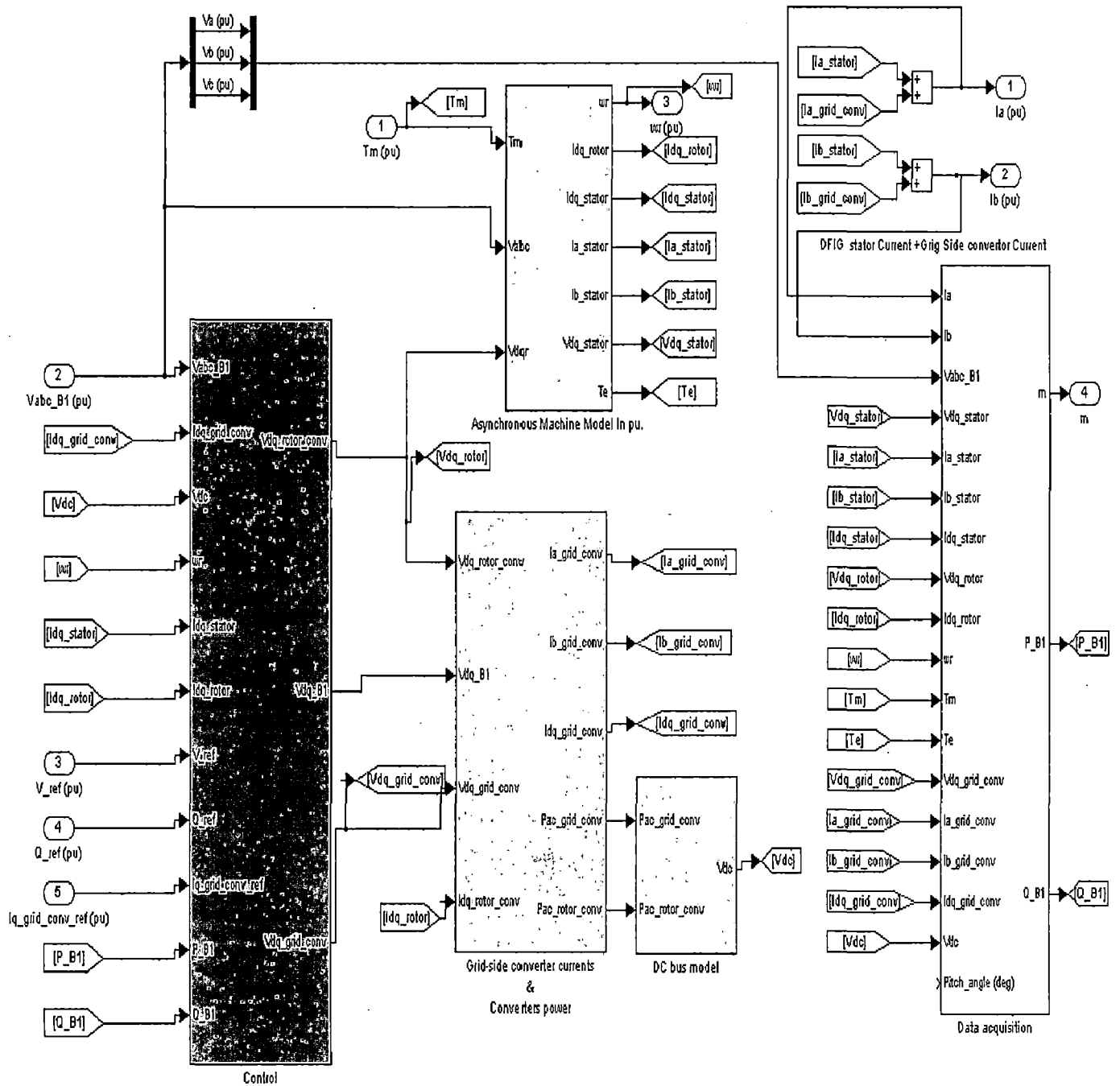
Fig. 4.2 MATLAB model of DFIG with rotor and stator side control
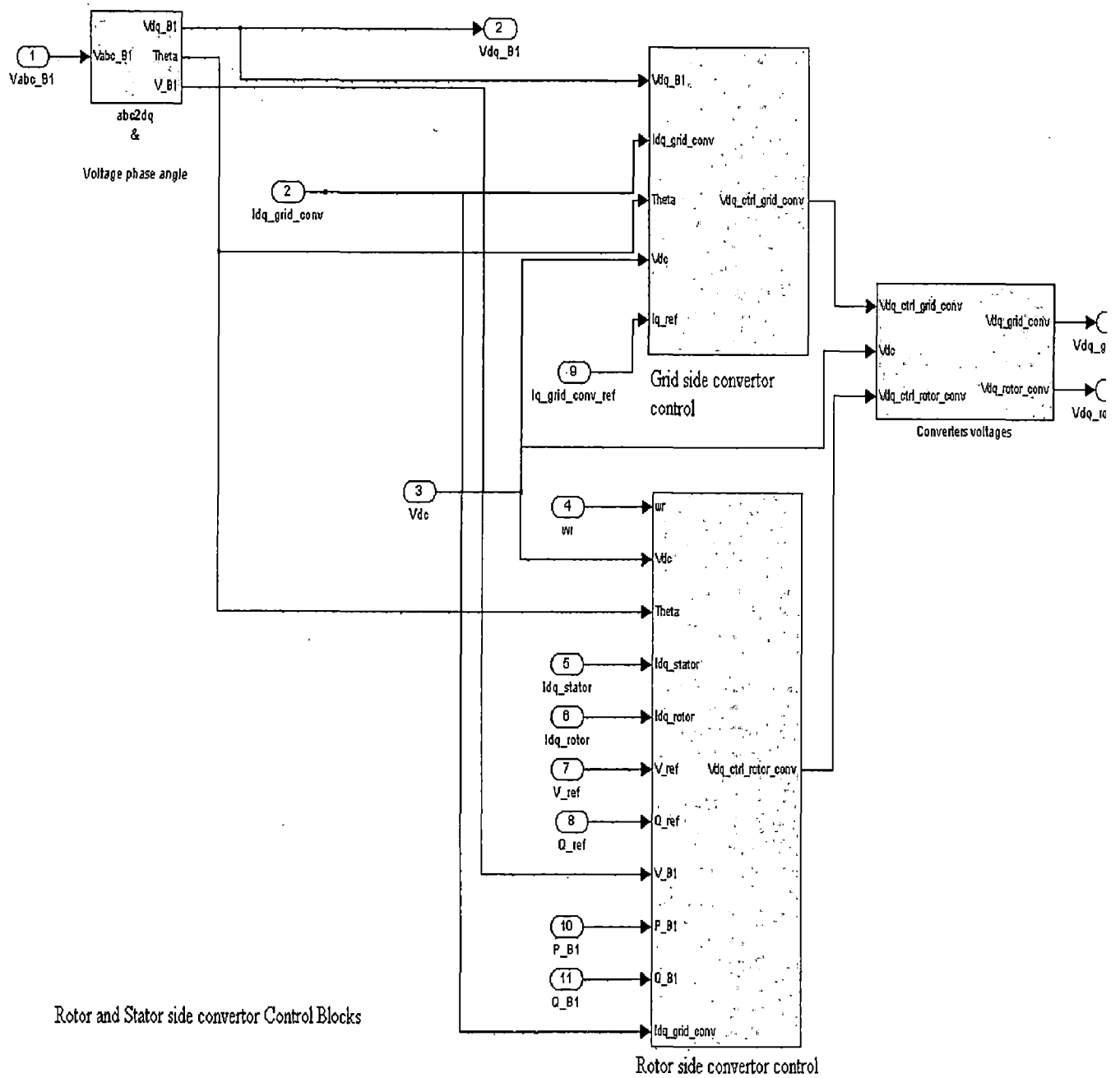
Fig. 4.3 Rotor and grid side convertor control blocks

is equal to P_r . The power control will be explained below. The phase-sequence of the AC voltage generated by Crotor is positive for sub-synchronous speed and negative for super-synchronous speed. The frequency of this voltage is equal to the product of the grid frequency and the absolute value of the slip. Crotor and Cgrid have the capability of generating or absorbing reactive power and could be used to control the reactive power or the voltage at the grid terminals.

4.2 C_rotor Control System

The rotor-side converter is used to control the Hydro turbine output power and the voltage (or reactive power) measured at the grid terminals.

4.2.1 Power Control

The generic power control loop is illustrated in the figure called "Rotor-Side Converter Control System" fig 4.6. The actual electrical output power, measured at the grid terminals of the Hydro turbine, is added to the total power losses (mechanical and electrical) and is compared with the reference power obtained from the tracking characteristic. A Proportional-Integral (PI) regulator is used to reduce the power error to zero. The output of this regulator is the reference rotor current Iqr_ref that must be injected in the rotor by convertor C_rotor. This is the current component that produce the electromagnetic torque T_{em} . The actual I_{qr} component of positive-sequence current is compared to Iqr_ref and the error is reduced to zero by a current regulator (PI). This is the current component that produce the output of this current controller is the

45
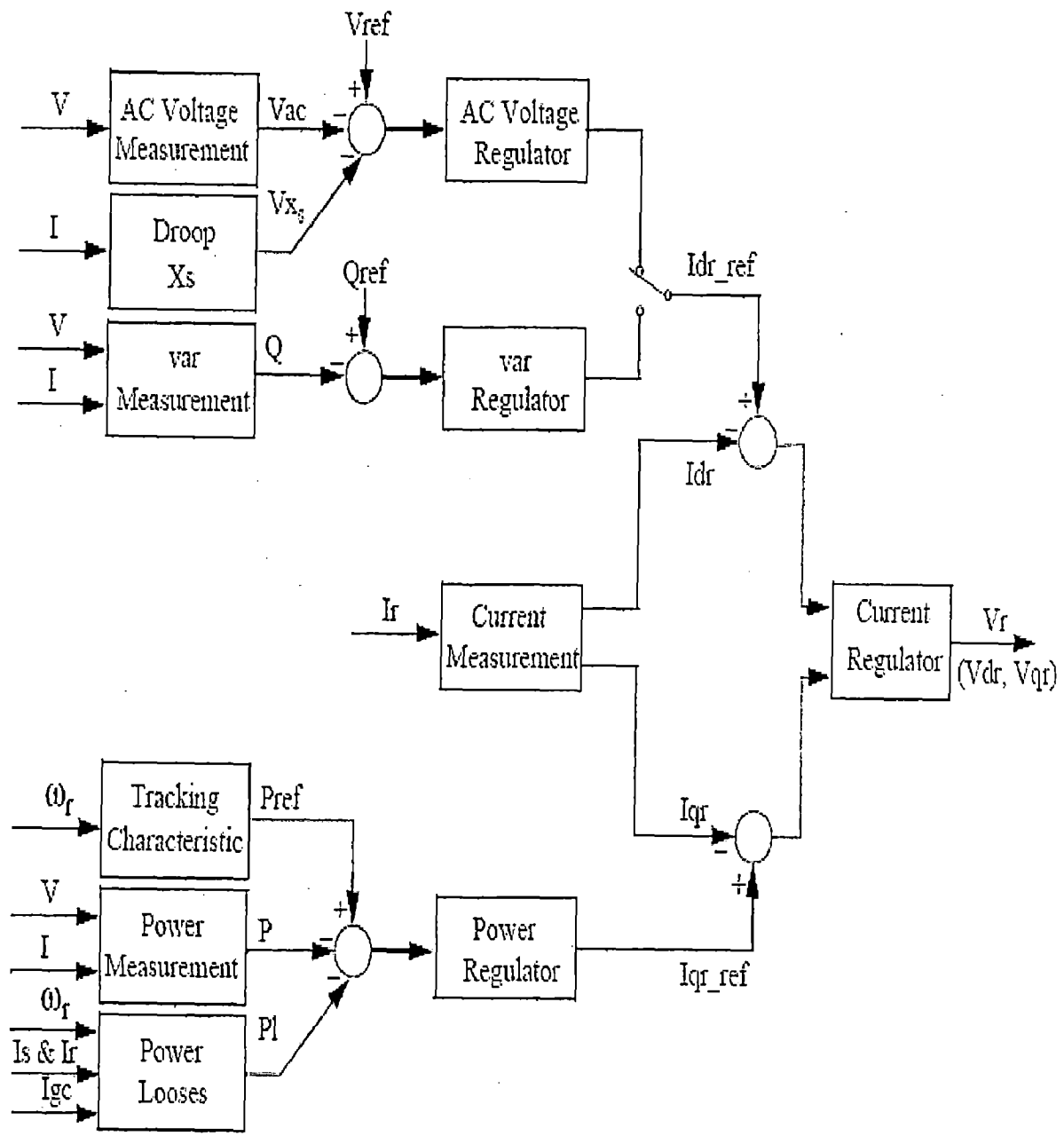
Fig 4.4 Rotor-Side Converter Control System

voltage Vqr generated by Crotor. The current regulator is assisted by feed forward terms which predict Vqr.

Rotor-side converter control system

Fig. 4.5 Rotor Side Convertor Control System

Fig.4.5 Rotor Side Convertor Control System

47
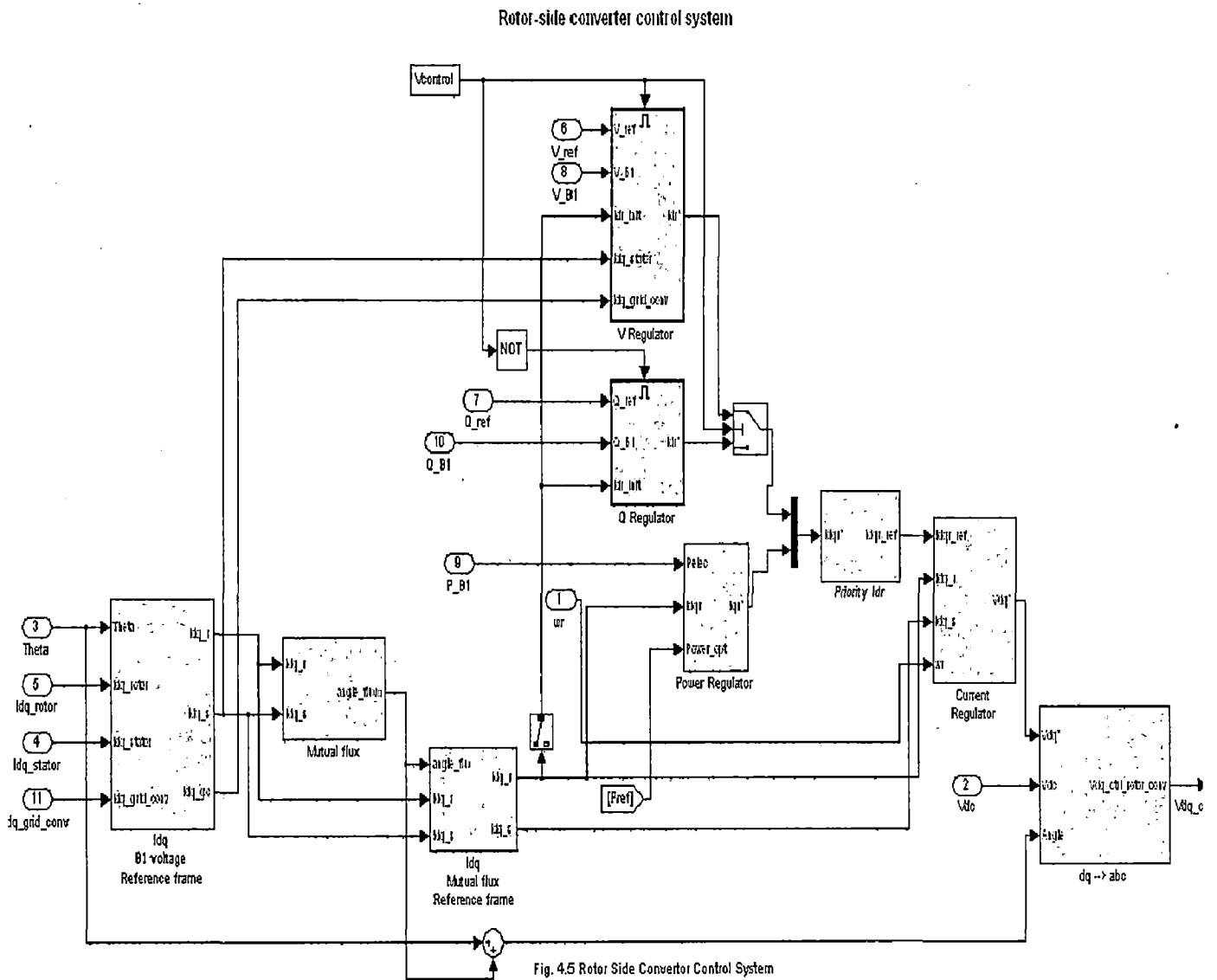
4.2.2 Voltage Control and Reactive Power Control

The voltage or the reactive power at grid terminals is controlled by the reactive current flowing in the converter Crotor. The generic control loop is illustrated in the figure called "Rotor-Side Converter Control System" in fig. 4.6 and MATLAB diagram is shown in figure 4.5. All sub blocks of the rotor side convertor control system are shown in Appendix.

When the system is operated in VAR regulation mode the reactive power at grid terminals is kept constant by a VAR regulator. The output of the voltage regulator or the VAR regulator is the reference d-axis current I_{dr_ref} that must be injected in the rotor by converter Crotor. The same current regulator as for the power control is used to regulate the actual Idr component of positive-sequence current to its reference value. The output of this regulator is the d-axis voltage V_{dr} generated by Crotor. The current regulator is assisted by feed forward terms which predict V_{dr}. V_{dr} and V_{qr} are respectively the d-axis and q-axis of the voltage V_r.

For Crotor control system and measurements the d-axis of the d-q rotating reference frame is locked on the generator mutual flux by a PLL which is assumed to be ideal in this phasor model.

The magnitude of the reference rotor current I_{r_ref} is equal to $\sqrt{I^2{}_{dr} + I^2_{qr}}$. The maximum value of this current is limited to 1 p.u. When I_{dr_ref} and I_{qr_ref} are such that the magnitude is higher than 1 p.u. the I_{qr_ref} component is reduced in order to bring back the magnitude to 1 p.u.

4.3 C_grid Control System

The converter Cgrid is used to regulate the voltage of the DC bus capacitor. In addition, this model allows using Cgrid converter to generate or absorb reactive power. The control system, illustrated in the figure called "Grid-Side Converter Control System" in fig. 4.6, consists of:

(a) Measurement systems measuring the d and q components of AC positive-sequence currents to be controlled as well as the DC voltage Vdc.

(b) An outer regulation loop consisting of a DC voltage regulator. The output of the DC voltage regulator is the reference current I_{dgc_ref} for the current regulator (I_{dgc} = current in phase with grid voltage which controls active power flow)
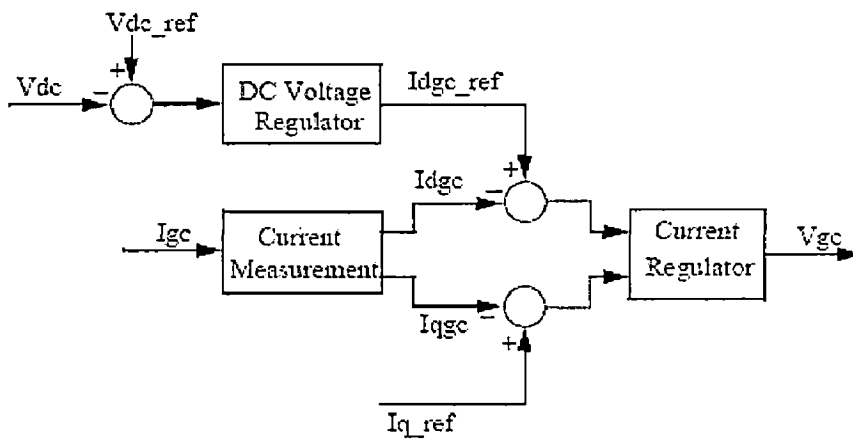
Fig. 4.6 Grid Side Converter Control System

An inner current regulation loop consisting of a current regulator. The current regulator controls the magnitude and phase of the voltage generated by converter Cgrid (Vgc) from the I_{dgc_ref} produced by the DC voltage regulator and specified I_{dgc_ref} I_{q_ref} reference.

The current regulator is assisted by feed forward terms which predict the Cgrid output voltage.

The magnitude of the reference grid converter current I_{gc_ref} is equal to $\sqrt{I^2_{qgc\_ref} + I^2_{qgc\_ref}}$. The maximum value of this current is limited to a value defined by the converter maximum power at nominal voltage. When I_{dgc_ref} and I_{q_ref} are such that the magnitude is higher than this maximum value ,the I_{q_ref} component is reduced in order to bring back the magnitude to its maximum value. MATLAB diagram of grid side convertor control system is shown in figure 4.7 and all of it's sub blocks are shown in appendix.

50
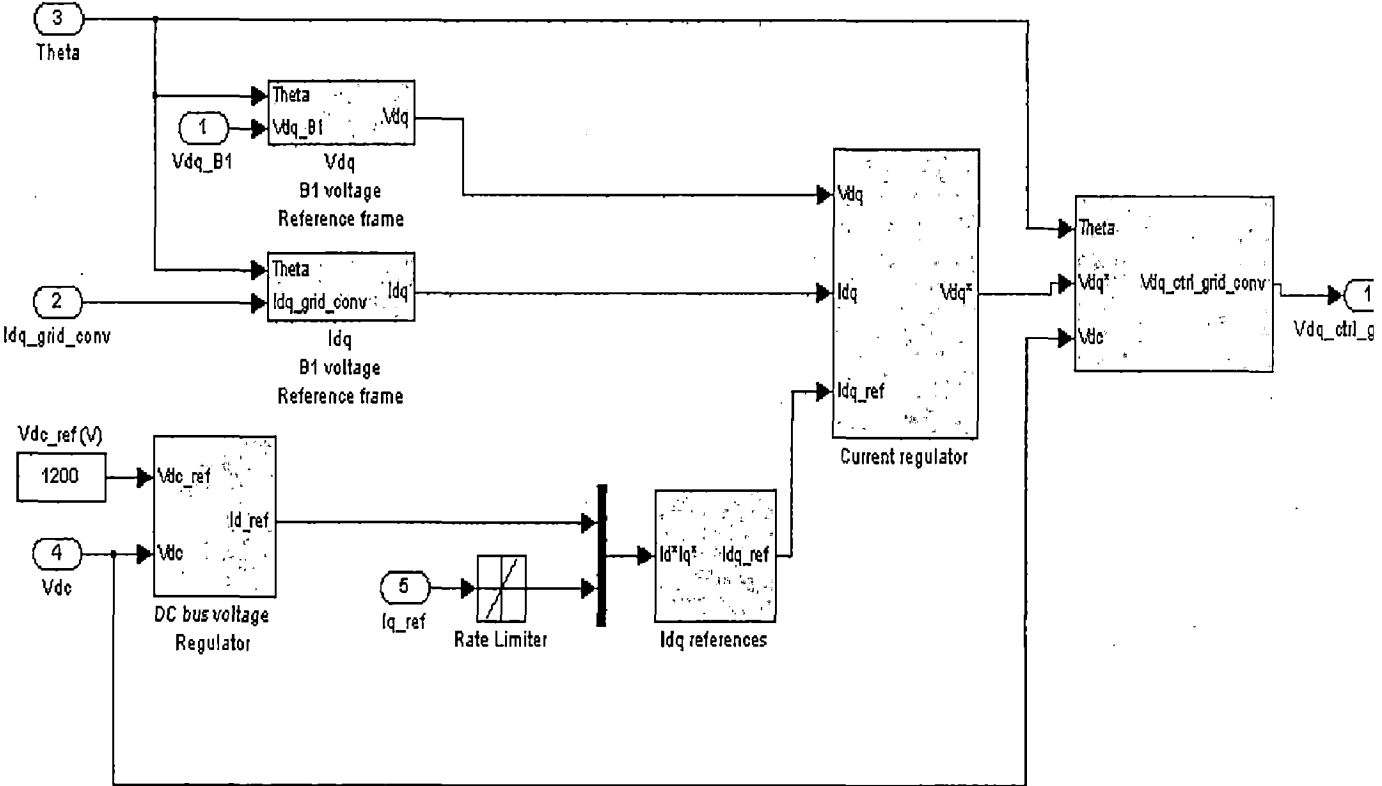
Fig 4.8 Grid side convertor control system

RESULT DISCUSSION

Parameters used to simulate the Doubly fed induction generator and hydraulic turbine system are as follows

5.1 DFIG Generator Parameters

Rated Power   = 12kVA

Rated Terminal Voltage of Stator   = 575

Rated Frequency   = 60Hz.

Stator resistance   Rs   = 0.00706 pu

Stator inductance Lls   = 0.171 pu

Rotor Resistance   Rr'   = 0.005   pu

Rotor Inductance   Llr'   = 0.156   pu

Mutual Inductance Lm   = 2.9   pu

Inertia constant H(s)   = 3.04   s

Friction Factor   = 0.01   pu

Pair of pole P   = 3

5.2 Parameters of hydraulic turbine

Servomotor gain Ka   =10/3

      time constant Ta   =0.07

Gate opening Limits

g_{max} =0.975 pu.

g_{min} =0.01 pu

Gate speed

vg_{max} = 0.1 pu/s

vg_{max} = -0.1 pu/s

Water starting time T_w =2.67 sec

Permanent Droop R_p = 0.05

Regulator constants

k_p =1.163

k_i =0.150

k_i =0.01
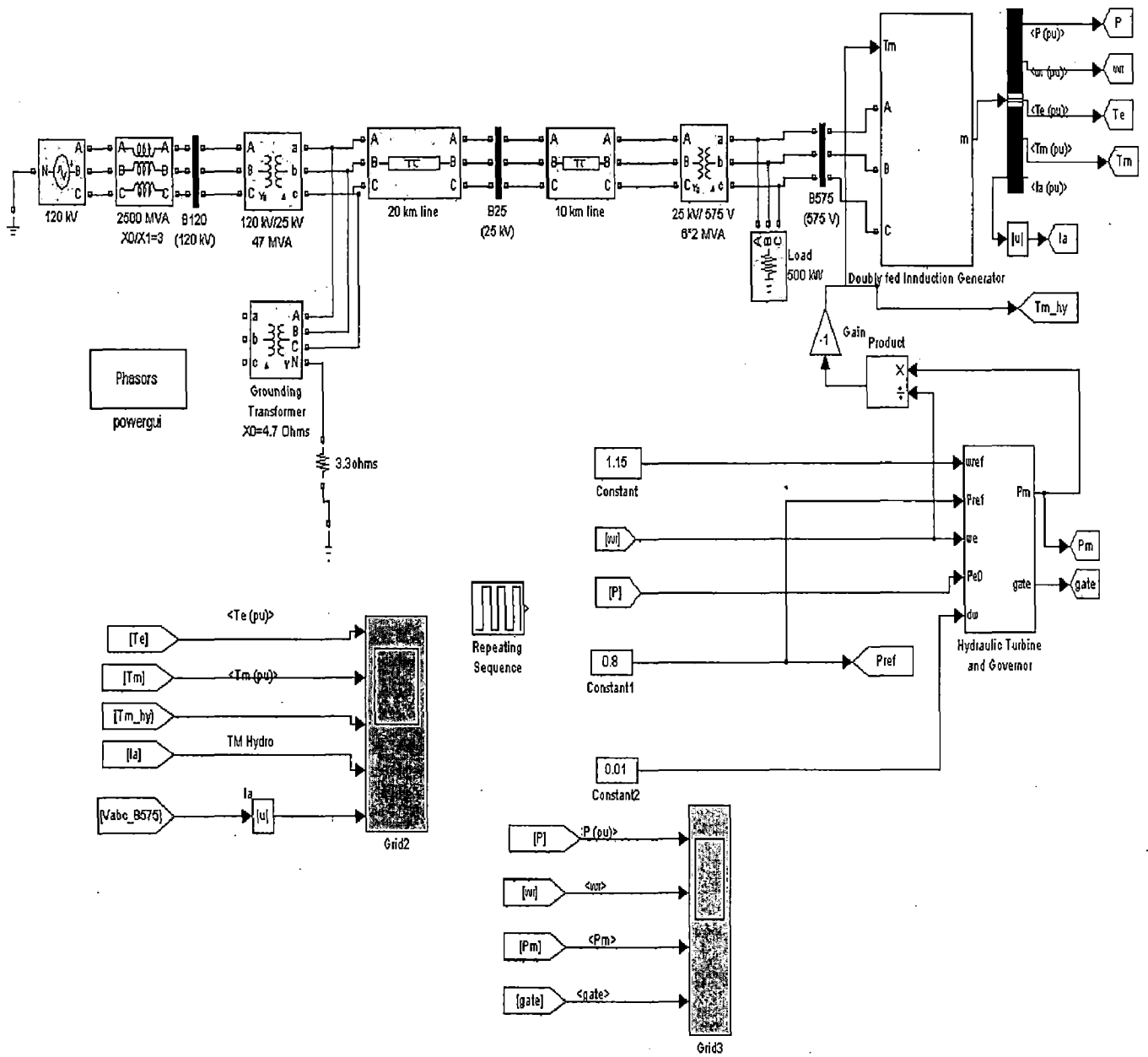
Fig. 4.2 Matlab circuit diagram for Doubly fed induction generator

54

5.3 Simulation Results :

MATLAB circuit diagram of a grid connected DFIG is shown in figure 5.1 A 10 MVA DFIG is connected to a 30 km 25Kv transmission line through 12 MVA (575V/25 kV) transformer and this transmission line is connected to 230kV grid.

The simulations of the dynamic responses to changes in mechanical power ,torque, reference turbine speed, are run and response is plotted out. The response includes plot of electromagnetic torque, the rotor speed in per unit, the current of the grid terminal, and the active and reactive power of the rotor and at the grid terminal.

Case a. Response for reference speed wr = 0.9(sub synchronous); and reference power varies as follows .

Time   = [0 50 50 80 100]

Reference power = [0.5 0.5 0.8 0.8]

When reference power of the turbine is varied from 0.4 pu (at t=0) to 0.5 pu its speed decreases below reference (0.9 pu) because of water inertia. And after 20 seconds it attains speed 0.9 pu. Response of gate opening and mechanical power variation is shown in figure 5.1(c). It is clear from the graph that at sub synchronous speed DFIG supplies active power to the grid and takes reactive power from the grid. From the figure it is clear that reactive power absorbed from the grid was initially 0.063 pu (0.63MVAr). when In response of step change in reference power (0.5 to0.8) it is changed to 0.08 pu. (0.8 MVAr) in 20 seconds. It is also clear that rotor takes both active and reactive power from the grid. Active power of rotor varies from -0.06 pu

to -0.1 pu and reactive power varies from -0.02 pu to -0.06 pu. Grid terminal voltage remains constant during operation.

Case b: Response for super synchronous speed .

Variation in reference power with time is as follows

Time   = [0 50 50 80 100]

Reference power = [0.5 0.5 0.8 0.8] p.u.

Response is shown in figure 5.2(b)

It is clear from the response (Fig. 5.2 (c)) that DFIG attains reference speed in 10 seconds. At super synchronous speed it supplies active power to the grid. Figure5.2(a) shows that rotor also supplies active and reactive power to the grid at super synchronous speed. Variation in mechanical power of turbine and gate opening is shown in figure 5.2(c).
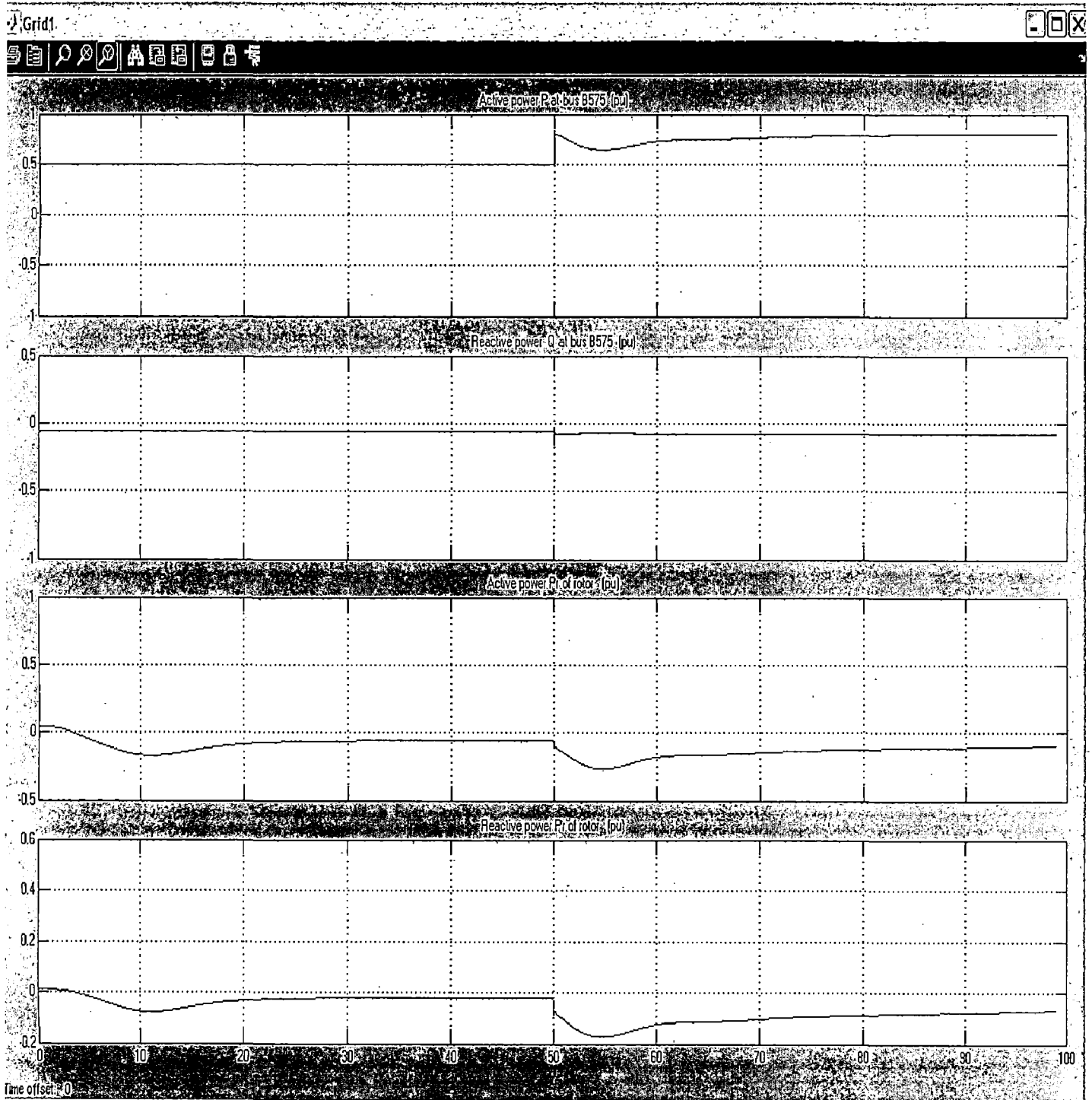
Fig. 5.1 (a) Variation in active and reactive power of DFIG during step change in reference power at sub synchronous speed
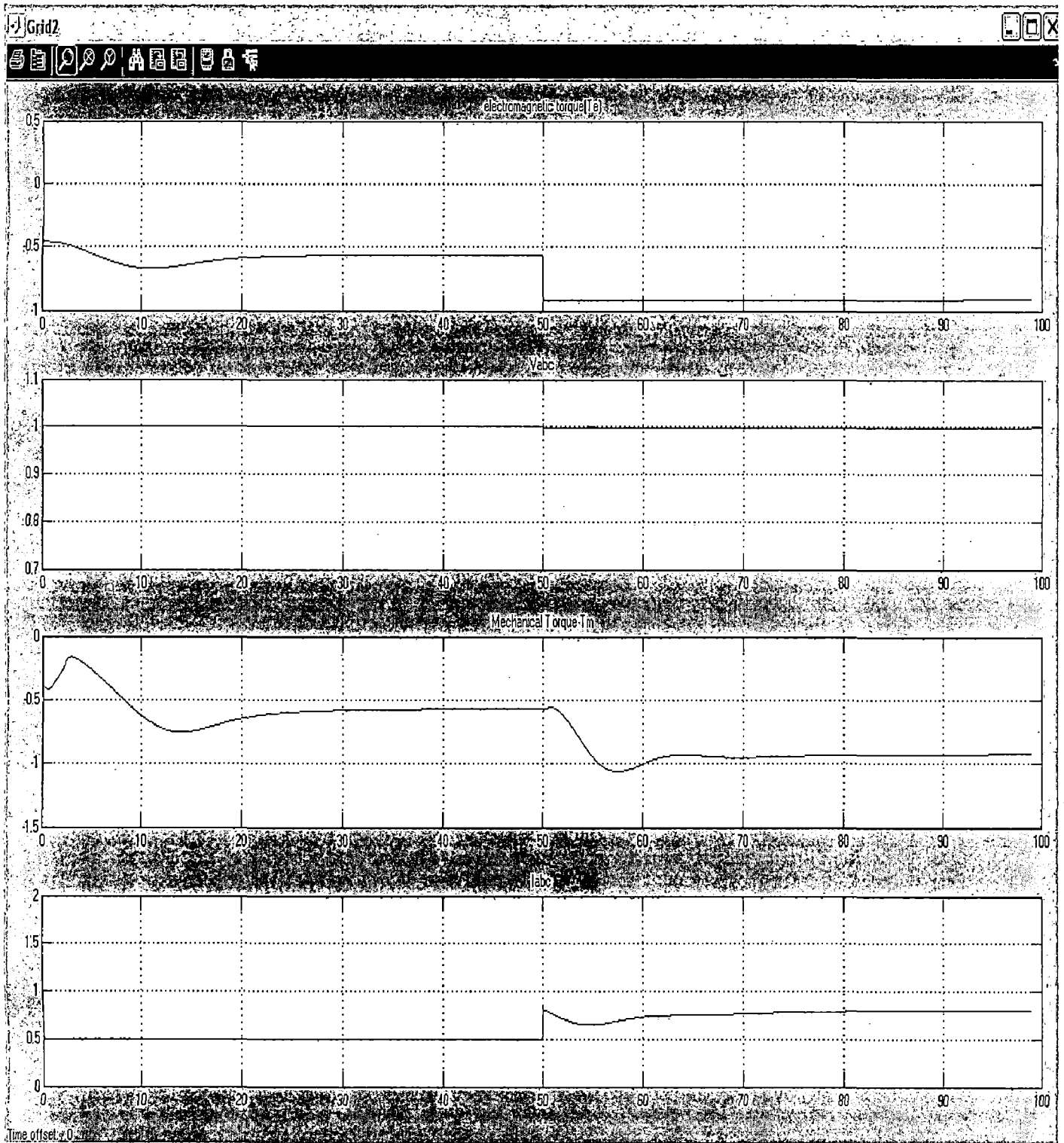
Fig. 5.1 (b) Variation in electromagnetic torque terminal voltage and current power of
DFIG during step change in reference power at sub synchronous speed

58
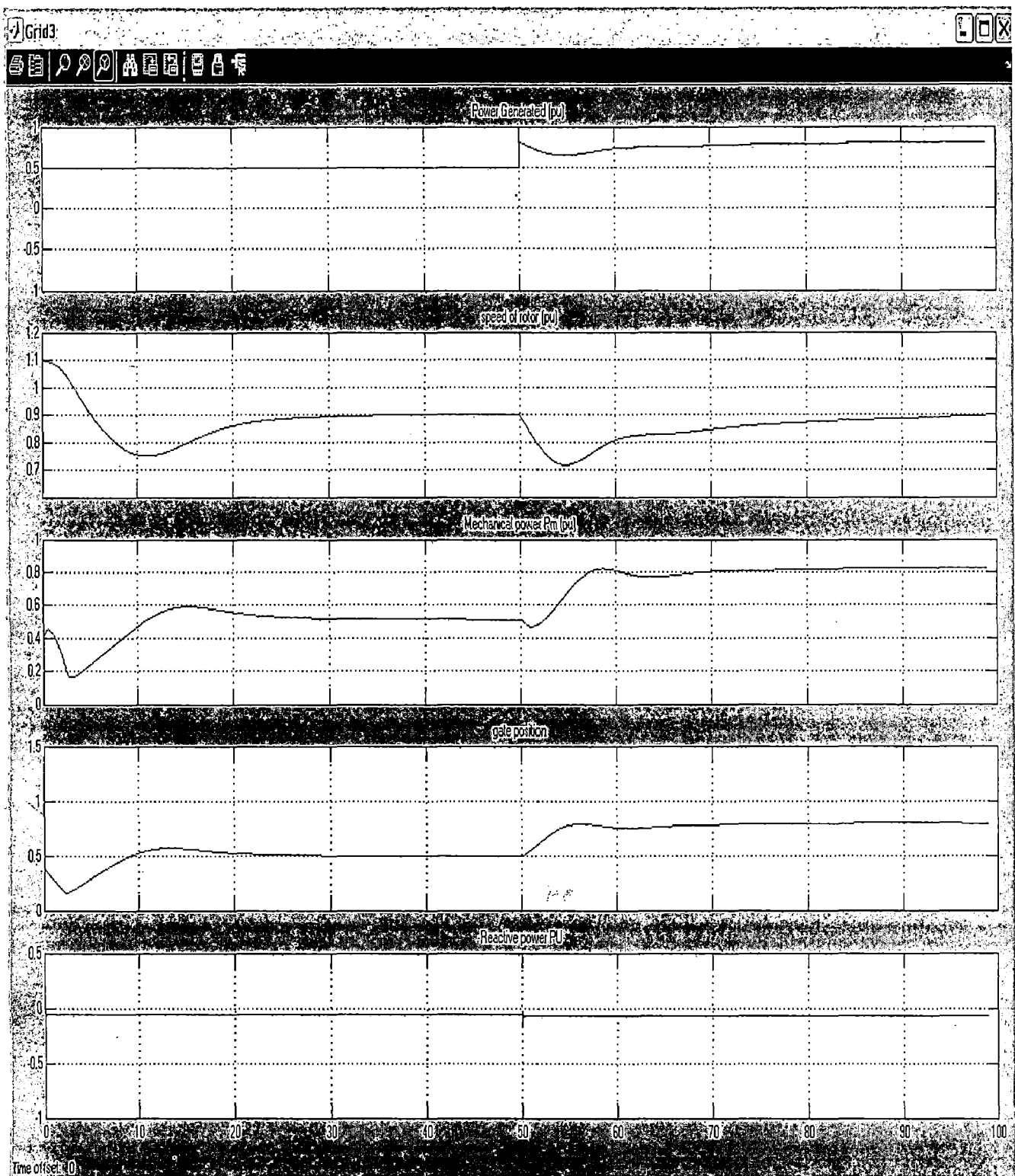
Fig. 5.1 (c) Variation in gate opening electromagnetic torque mechanical power, and speed   DFIG and hydraulic turbine during step change in reference power at sub synchronous speed
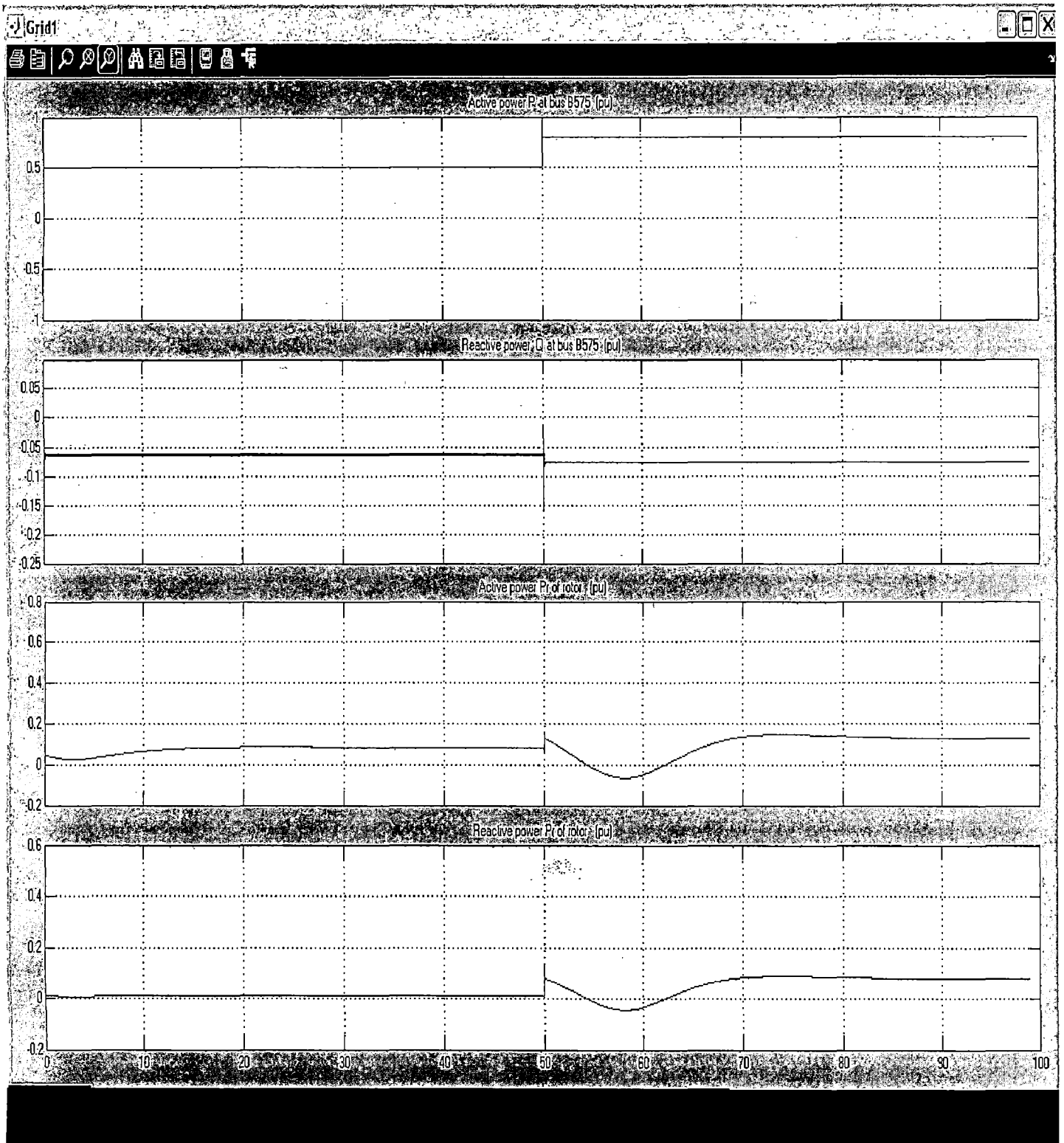
Fig. 5.2 (a) Variation in active and reactive power of DFIG during step change in reference power at super synchronous speed (wr* = 0.9 Pu)

60
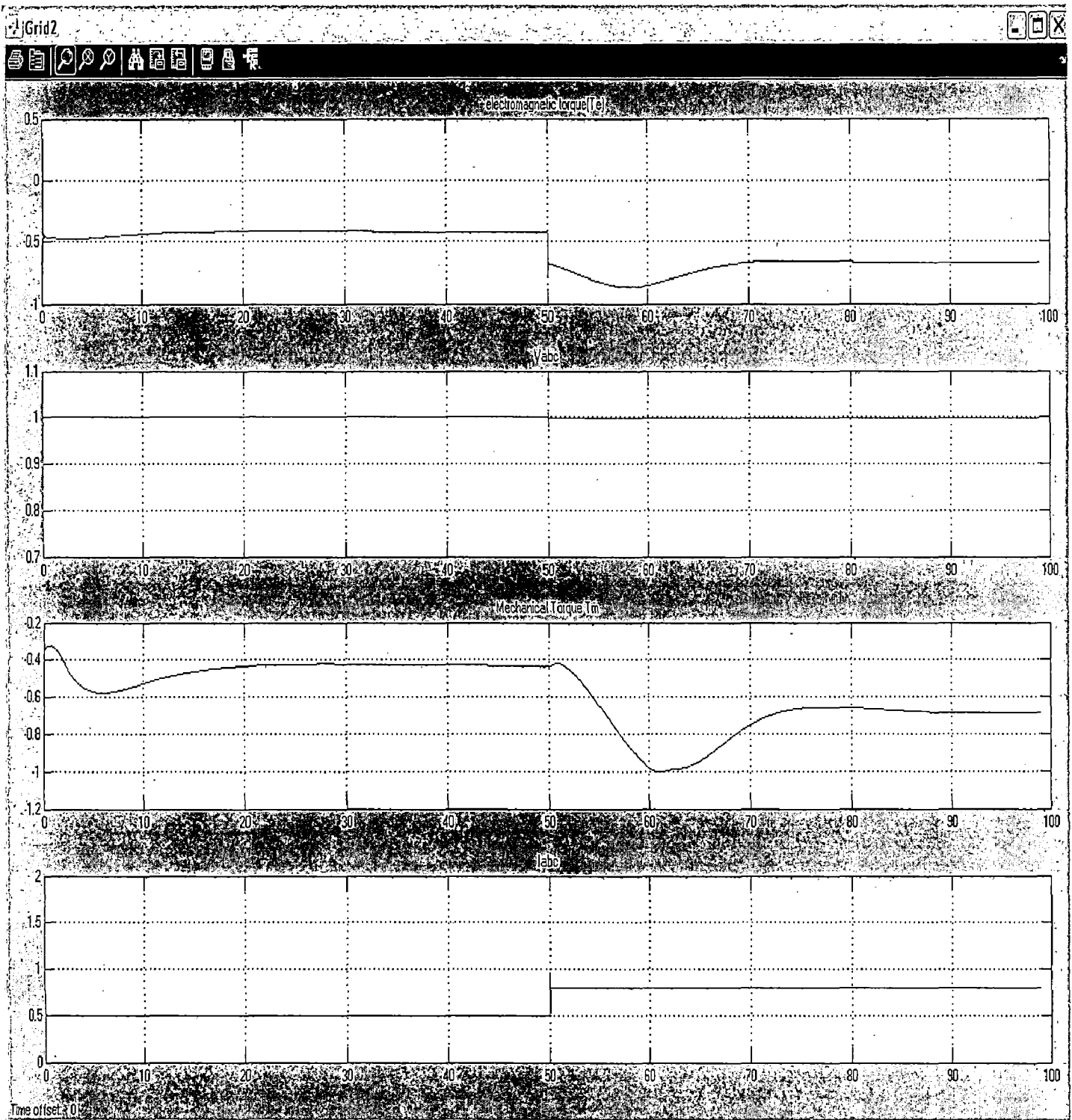
Fig. 5.2 (b) Variation in electromagnetic torque terminal voltage and current power of DFIG during step change in reference power at super synchronous speed (wr*=1.2 pu)
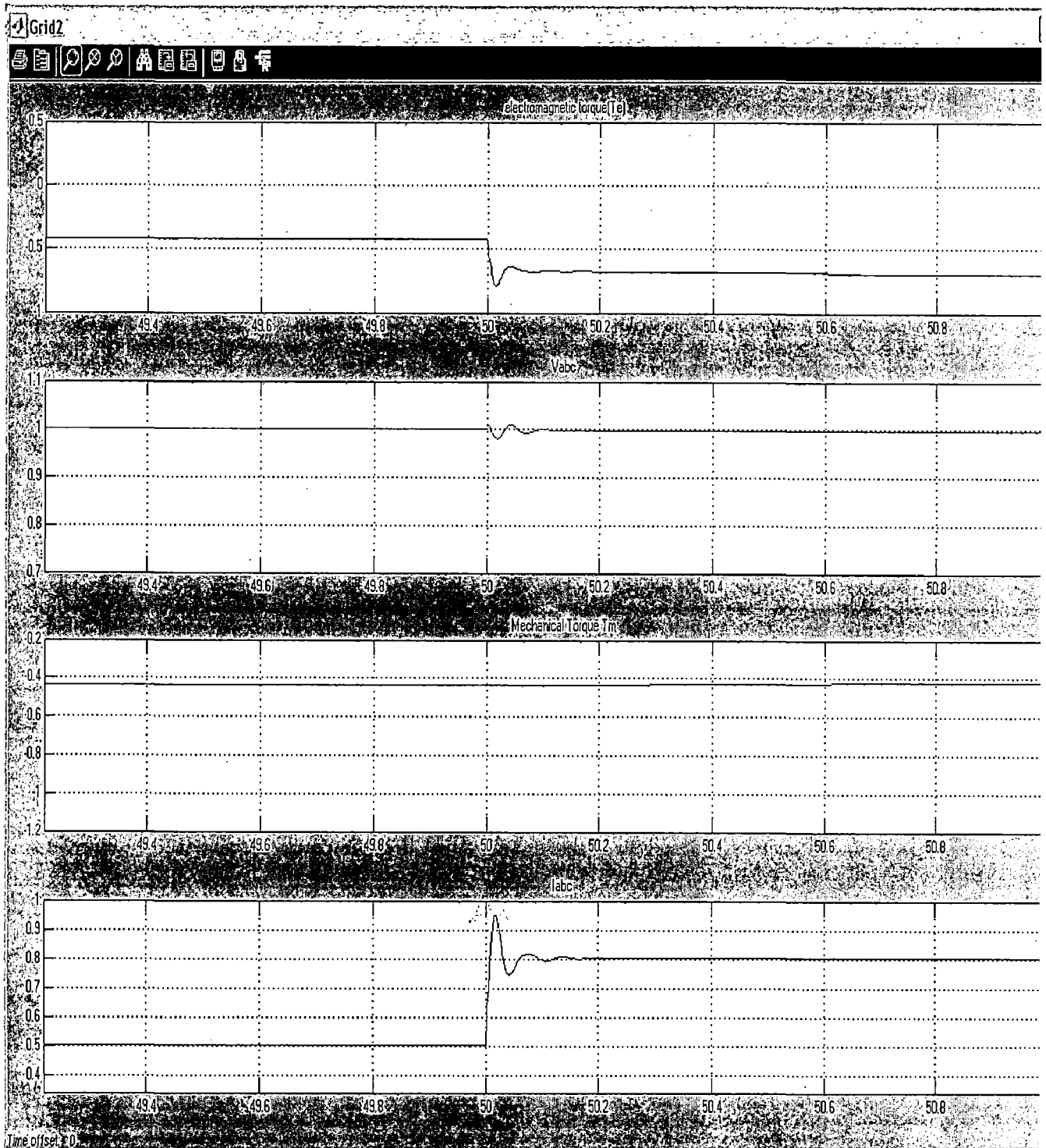
Fig. 5.2 .1(b) Variation in electromagnetic torque terminal voltage and current power
of DFIG during step change in reference power at super synchronous speed (wr*=1.2 pu)

62
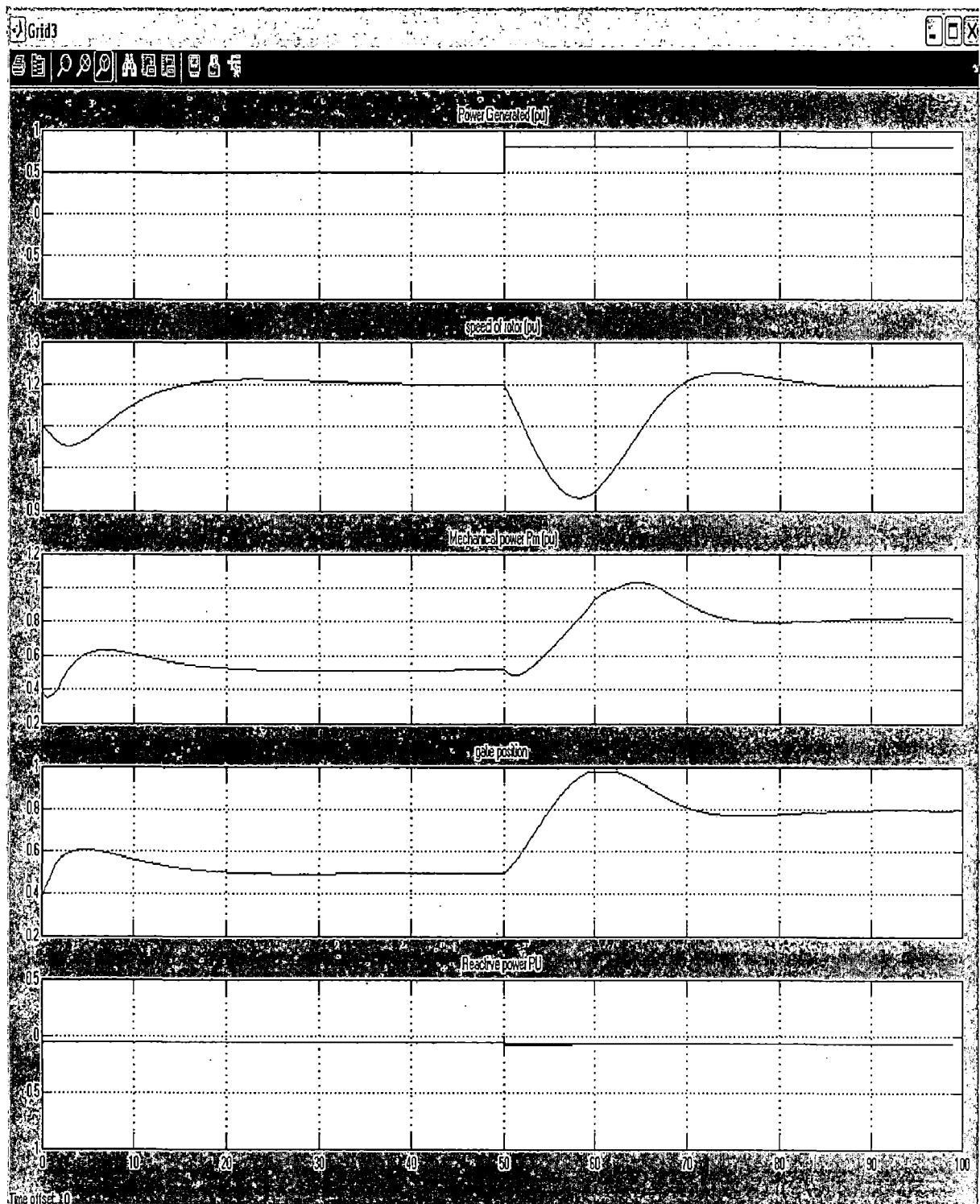
Fig. 5.2 (c) Variation in gate opening electromagnetic torque mechanical power, and speed DFIG and hydraulic turbine during step change in reference power at super synchronous speed (wr*=1.2 pu)

CONCLUSION

Various schemes for variable speed generation by Induction Generators for SHP are available in literature. In the present work, Doubly Fed Induction Generator with AC/DC/AC convertors has been considered. Model of Hydraulic Turbine and governor was used to simulate variable speed conditions. In SHP plants variable speed operation offers advantages which are based essentially on the greater flexibility of the turbine operation in situations under wide range of flow variation.

Following conclusions are drawn from the study:

1   It is found that operating range of the turbine can be increased with variable flow conditions in run-of-river based SHP schemes. Part load efficiency is increased by running turbine at required speed at different discharge conditions according to characteristic of the turbine.

2.   Power flow is examined on sub synchronous and super synchronous speeds. It has been found that at super synchronous speed operation active power is supplied to the grid by stator and rotor both. Thus it can generate active power more than its rated value without overheating . At super synchronous speed rotor supplies reactive power to the grid.

3.   At sub synchronous speed operation stator supplies active power to the grid and rotor absorbs active power from the grid. At sub synchronous speed stator and rotor both receive reactive power from the grid.

Future Scope of study

1. Variable speed generation can be very useful in variable head conditions. Effect of variable speed generation on efficiency can be studied in future study.

2. FACTs devices can be used to control reactive power in variable speed generation. This can also be scope of future study.

REFERENCES

1. Sheldon, L. H., "Analysis of the Benefit to be gained by using variable speed generator on Francis turbines," DOE/EPRI Variable speed generator workshop Hydro Applications, USBR Denver Federal Center, May 24-26, 1983.

2. Sheldon, L. H., "Analysis Of the Applicability and benefits of Variable Speed Generation for Hydro Power"

3. Bard, J. and Ritter, P., 'Variable speed operation in small hydro', Medium/Small hydro power & equipment, 2, 41-46, 1999

4. Grotenburg K., Bachmann,U. "Modeling and Dynamic Simulation of Variable Speed Pump Storage Units incorporated into the German Electric Power System" epe 2001 – graz

5. Jes´us Fraile-Ardanuy, Jos´e Rom´an Wilhelmi, Jos´e Jes´us Fraile-Mora, Senior, and Juan Ignacio P´erez. at el. "Variable-Speed Hydro Generation: Operational Aspects and Control" IEEE transactions on energy conversion, vol. 21, no. 2, june 2006

6. Soens, J., Karel de Brabandere, Driesen,J., Belmans. R., "Doubly Fed Induction Machine: Operating Regions and Dynamic Simulation". EPE 2003 Toulouse

7. Cadirci, I. Ermiq, M., "Double-output induction generator operating at sub synchronous and super synchronous speeds: steady-state performance optimization and wind-energy recovery". IEE proceedings-b, september 1992 Vol. 139, No. 5 429-442.

8. Pena, R., Clare, J.C., Asher, G.M. at el ."Doubly fed induction generator using back-to-back PWM converters and its application to variable speed wind-energy generation" IEE Proc.-Electr. Power Appr., May 1996 Vol. 143, No 3, 231-241.

9. Fraile-Ardanuy, J., Wilhelmi, J.R., J. Fraile-Mora, J. I. Pérez and I. Sarasúa "A dynamic model of adjustable speed hydro plants" 9 Congreso Hispano Luso de In

10. Krause, P. C., Wasynczuk. O., Sudhoff, S. D. "Analysis of Electrical Machine and Drive Systems IEEE press series on power Engineering", IEEE Press, John Wiley and Sons, Inc Publication.geniería Eléctrica, Marbella (España), 30 Junio a 2 de Julio de 2005

11. Chaudhry M.H., , Applied Hydraulic Transients, Van Nostrand, 1979.

12. Farrell C. and Gulliver, J. "Hydromechanics of variable speed turbines," J Energy Eng., ASCE, vol. 113, no. 1, pp. 1–13, May 1987.

13. J. G. C. Barros, M. A. Saidel, L. Ingram, and M.Westphalen, "Adjustable speed operation of hydroelectric turbine generators," Electra, no. 167, pp. 17–36, Aug. 1996.

14. L. Cuesta and E. Vallarino, Aprovechamientos Hidroeléctricos. vol. 15. Madrid: Colegio de Ingenieros de Caminos, Canales y Puertos, 2000.

15. J. M. Merino and A. López, "ABB varspeed generator boosts efficiency and operating flexibility of hydropower plant," ABB Rev., no. 3, pp. 33–38, 1996.

16. M. Ermis, "Various induction generator schemes for wind-electricity generation", Electric Power System Research, Vol. 23, 1992, pp. 71 -83.

17. H. L. Nakra, "Slip power recovery induction generators for large vertical axis wind turbines." IEEE Trans. Energy Conversion, Vol. 3, No. 4, Dec. 1988, pp. 733-737,

18. Longya Xu and Wei Cheng, "Torque and reactive power control of a double fed induction machine by position sensor less scheme," IEEE Trans. Indu. Appl., Vol. 3 1, No. 3, May/June 1 995, pp. 636-642.

19. . Ai Zahawi, B.A.T, B.L. Jones and W. Dniry, "Analysis and simulation of static Kramer drive under steady-state conditions," IEE Proc. Vol. 136, Pt. B, No. 6, Nov. 1989, pp. 28 1-291.

20. Uctug, M.Y., 1 Eskandarzadeh and H. Ince, "Modeling and output power optimization of a wiod turbine drive double output induction generator," IEE Proc.-Electr. Power Appl., Vol. 14 1, No.2, March 1994.

21. Murphy. J.M.D., & FG Turnbull, "Power Elecdc Control of AC Motor," Pergamon Press, 1988.

22. www.mathswork.com

23. Sothi N. ,"Three phase self excited induction generator feeding single phase load" M. E. Dissertation thesis ,Alternate Hydro Energy Centre, IIT Roorkee,2001
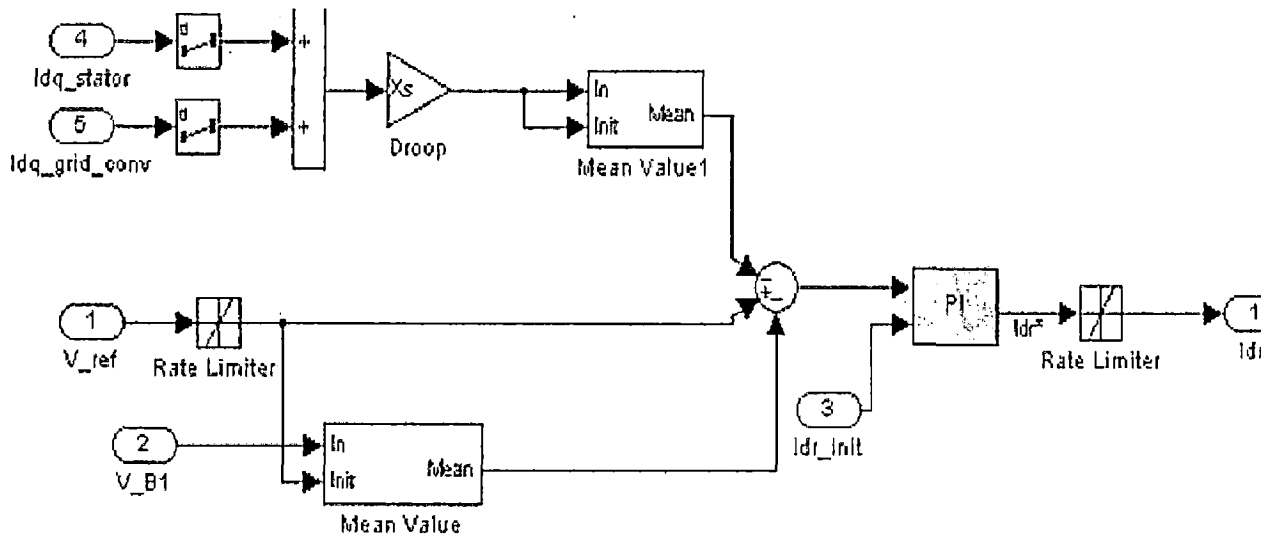
Fig. A.1. Rotor side convertor voltage regulator

Fig.
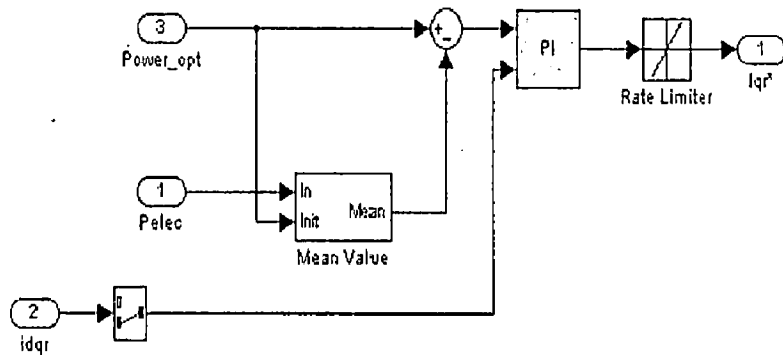
A.2. Rotor side convertor Power regulator
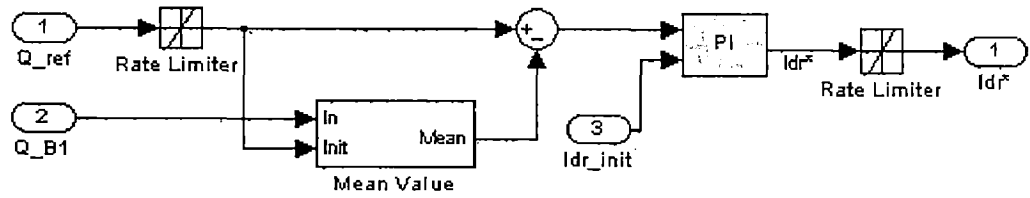
Fig. A.3. Rotor side convertor Q regulator
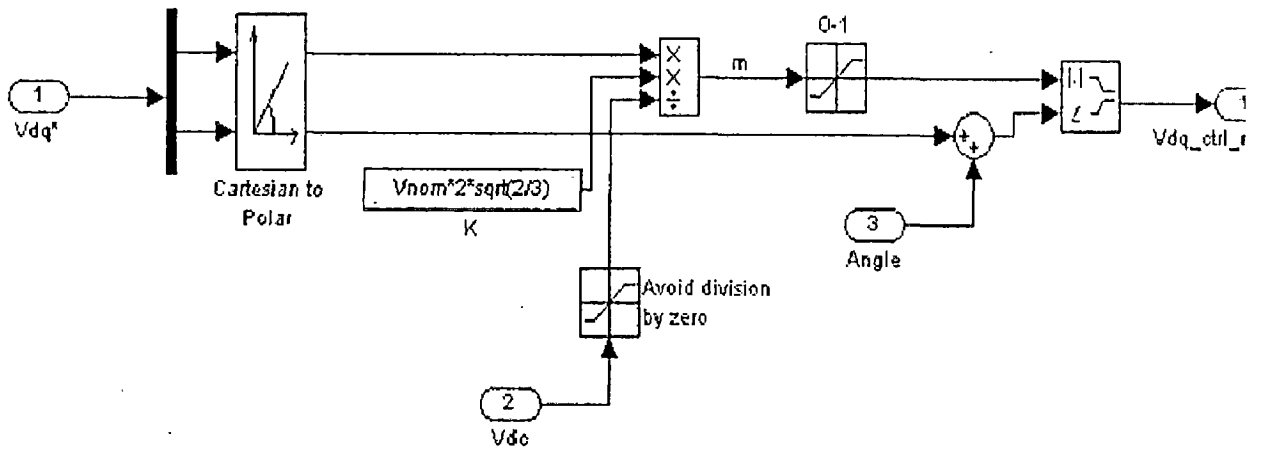
Fig. A.4. Rotor side convertor block to obtain 1 pu generated voltage by convertor
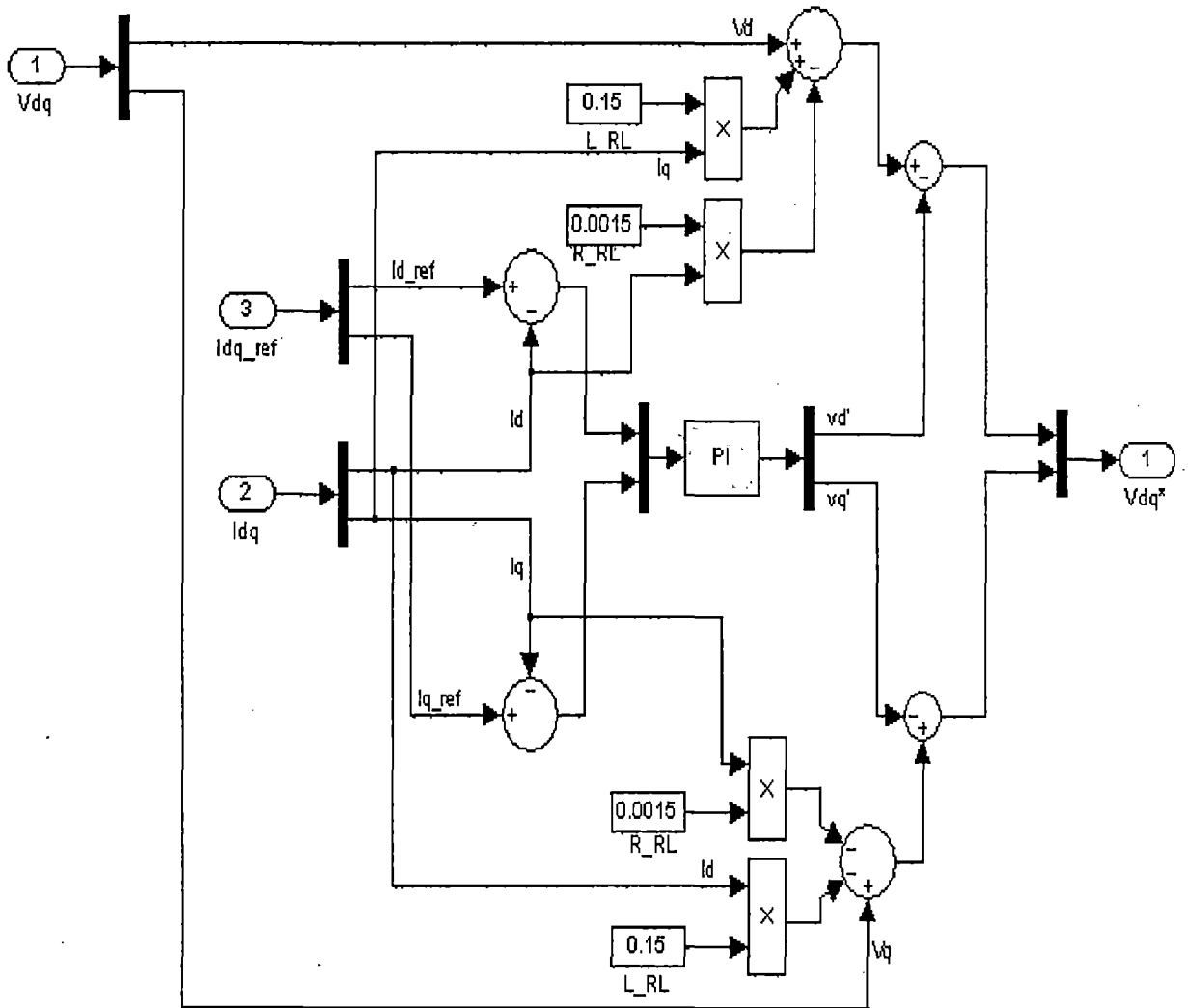
Fig. A.5. Rotor side convertor block current regulator
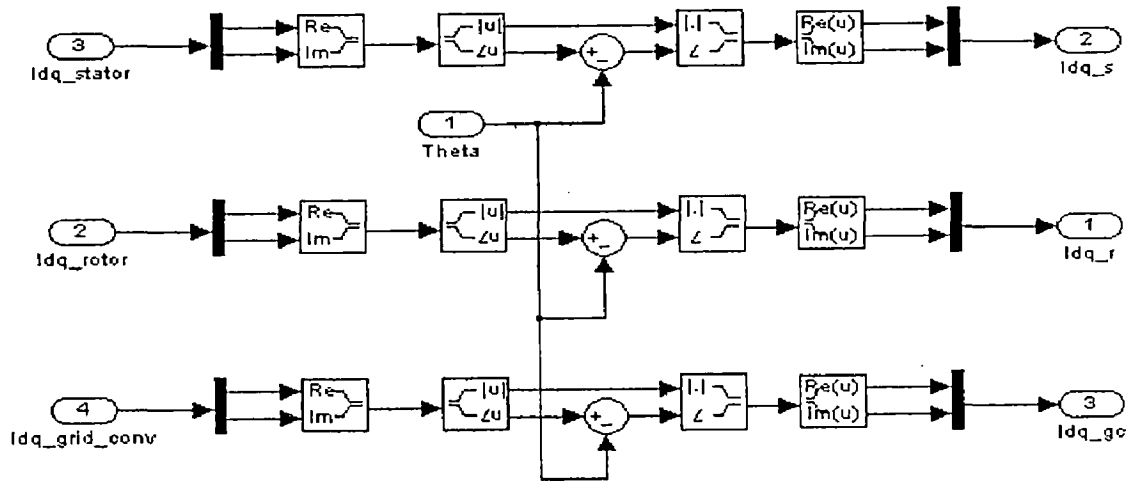
A.6. Rotor side convertor Idq voltage reference frame
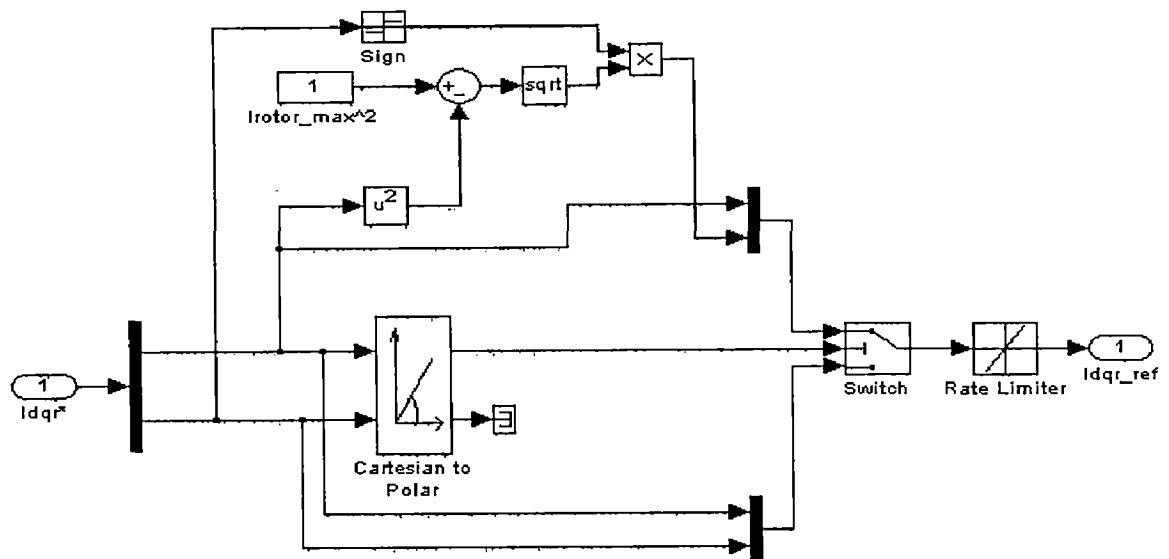
Fig. A7. Priority Idr Rotor side convertor

72
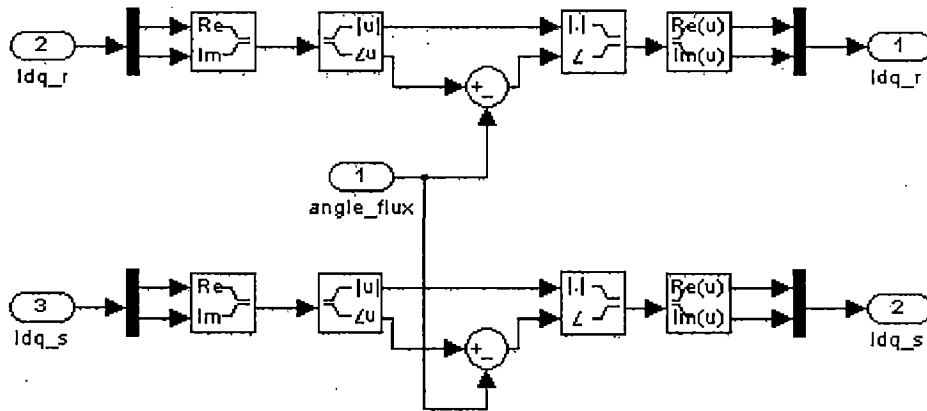
Fig. A .8. Idq Mutual flux Reference frame
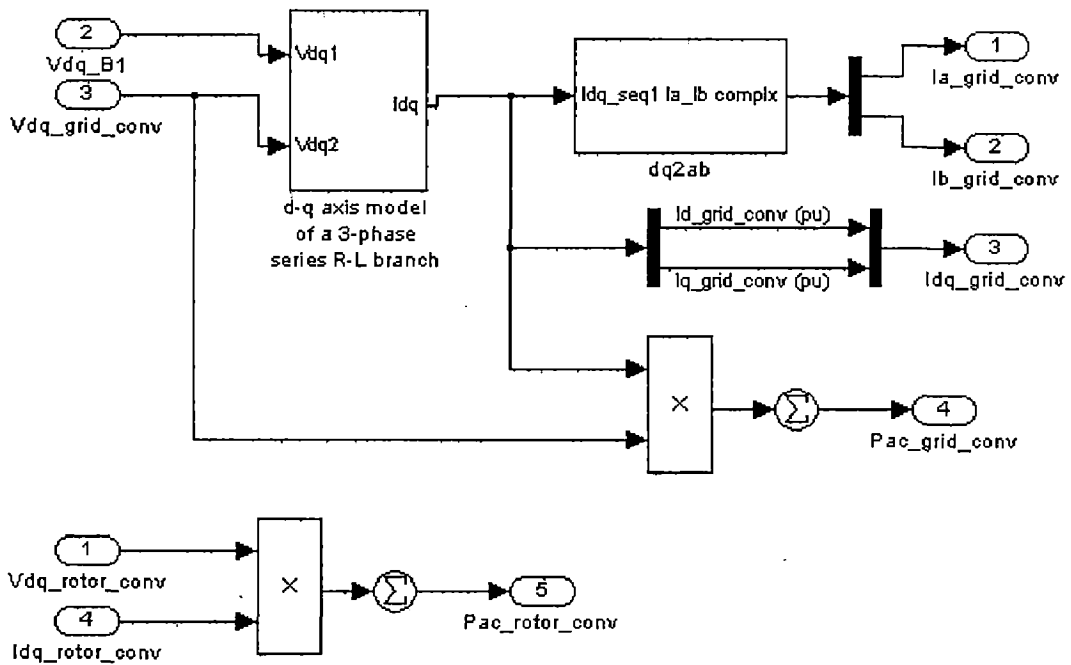
Fig. A .9. Grid side convertor current and convertor power
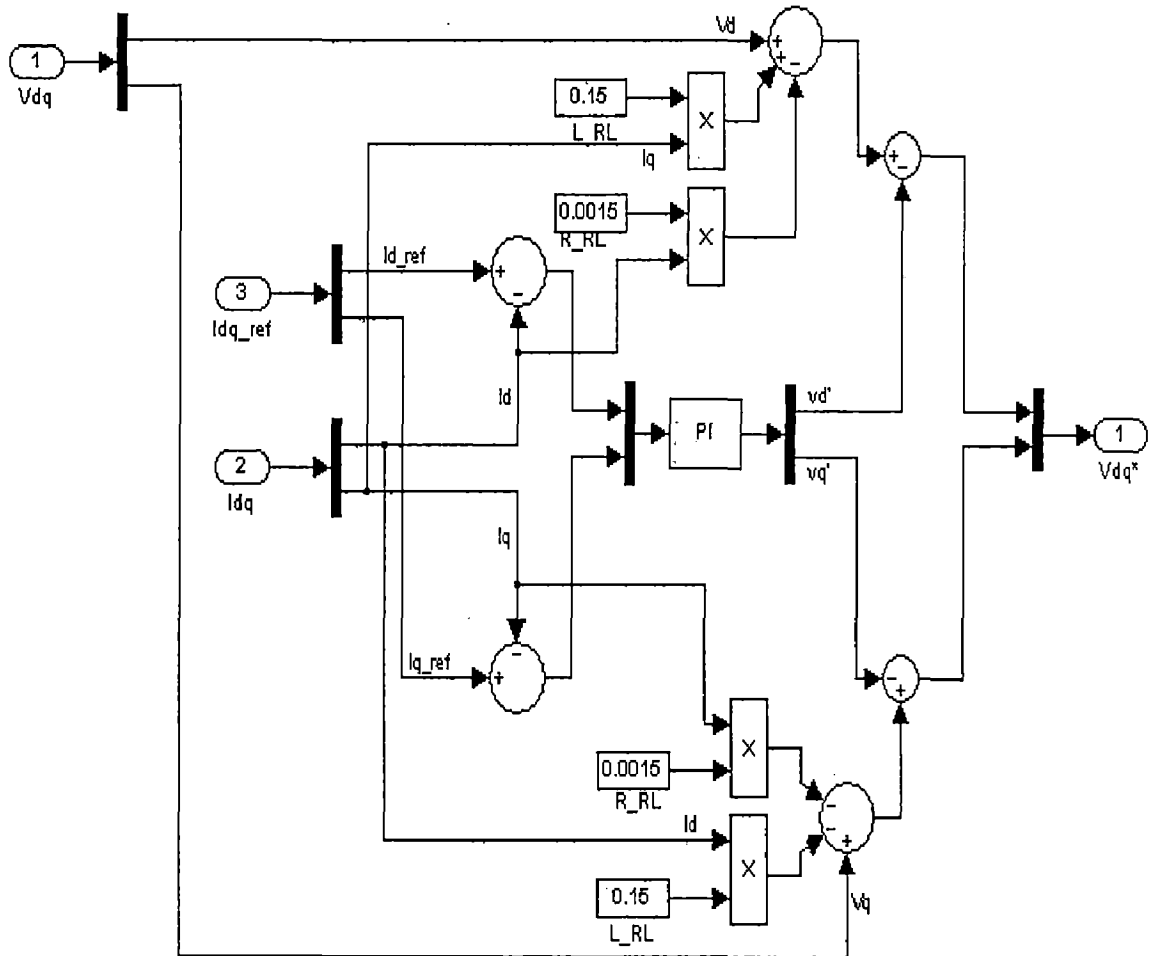
Fig. A .10. Grid side convertor current regulator
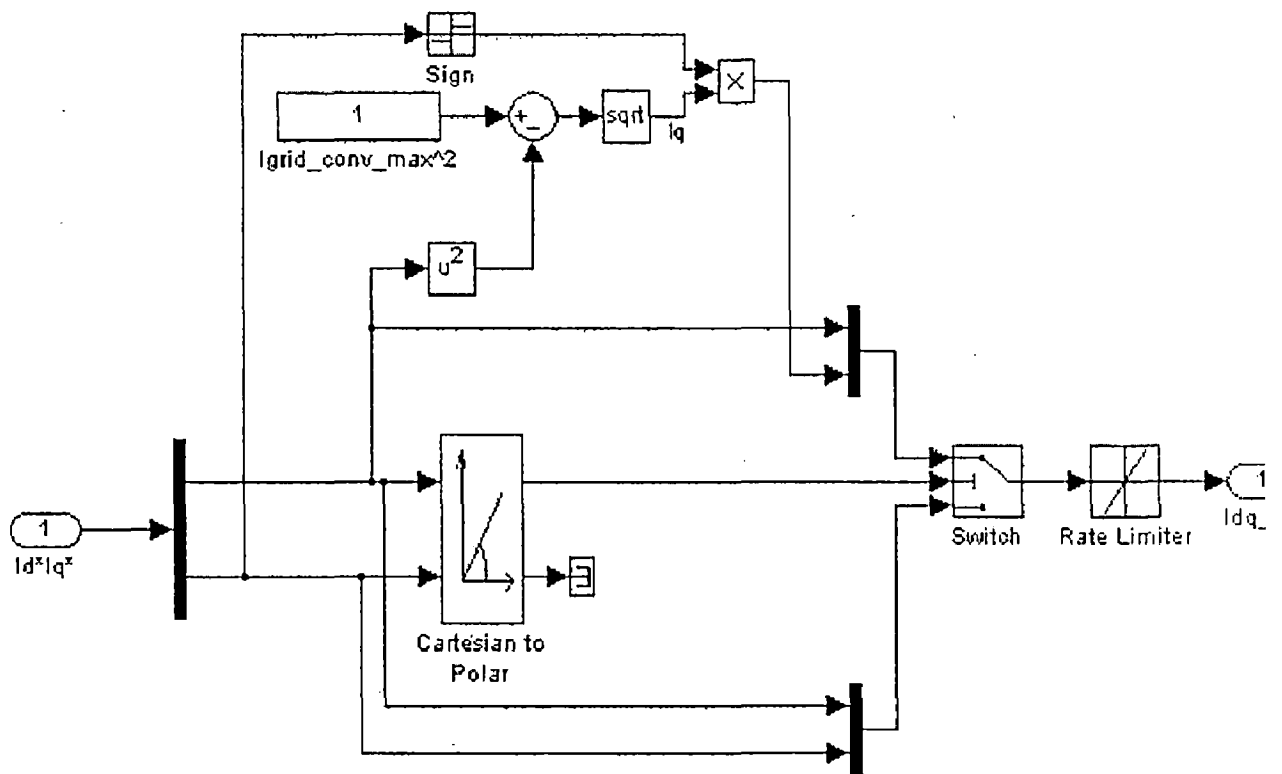
Fig. A.11 Idq reference for Grid side convertor
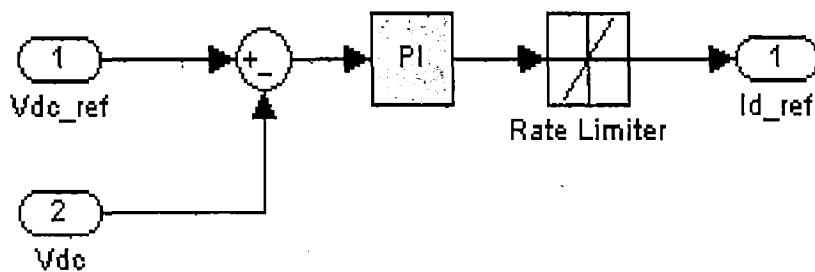
Fig. A.12 DC bus voltage regulator for Grid side convertor
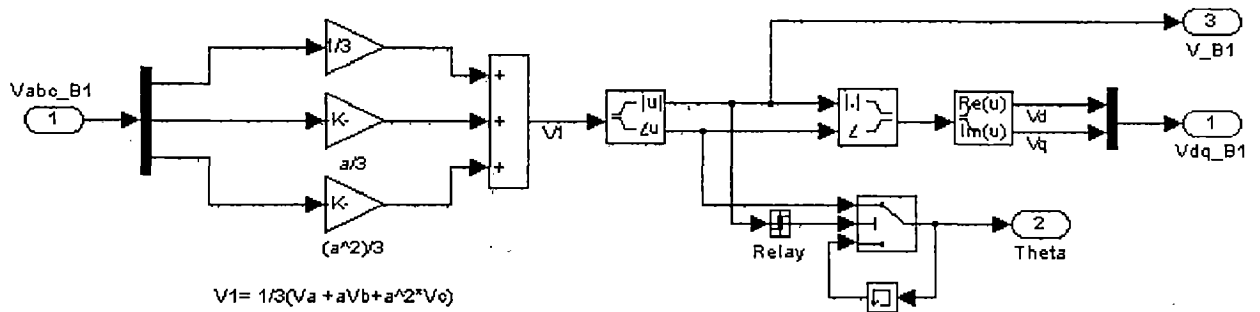
Fig. A.13   abc2dq & Positive sequence Voltage phase angle

Fig. A.14   Model of induction generator

76
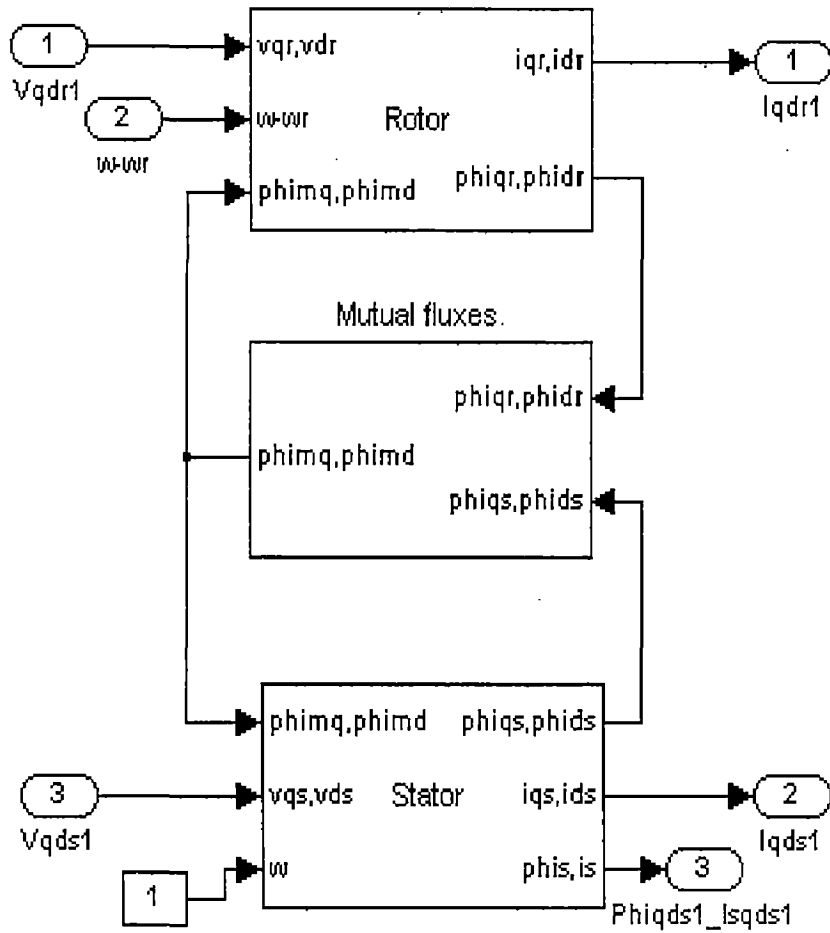
Fig. A.14 Model of induction generator (positive sequence)
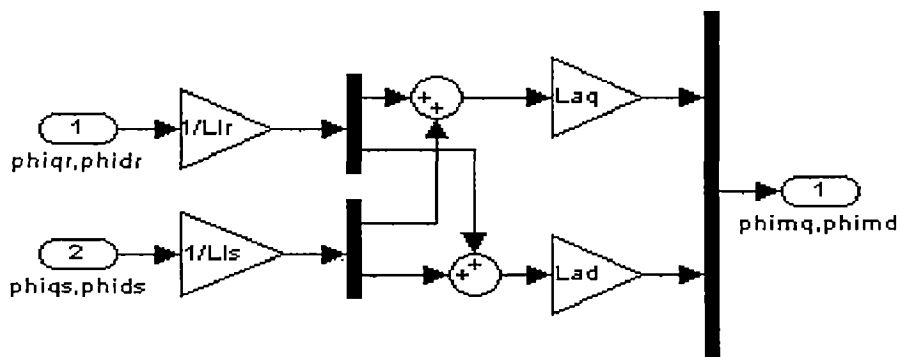
Fig. A.15 Mutual flux model for induction generator
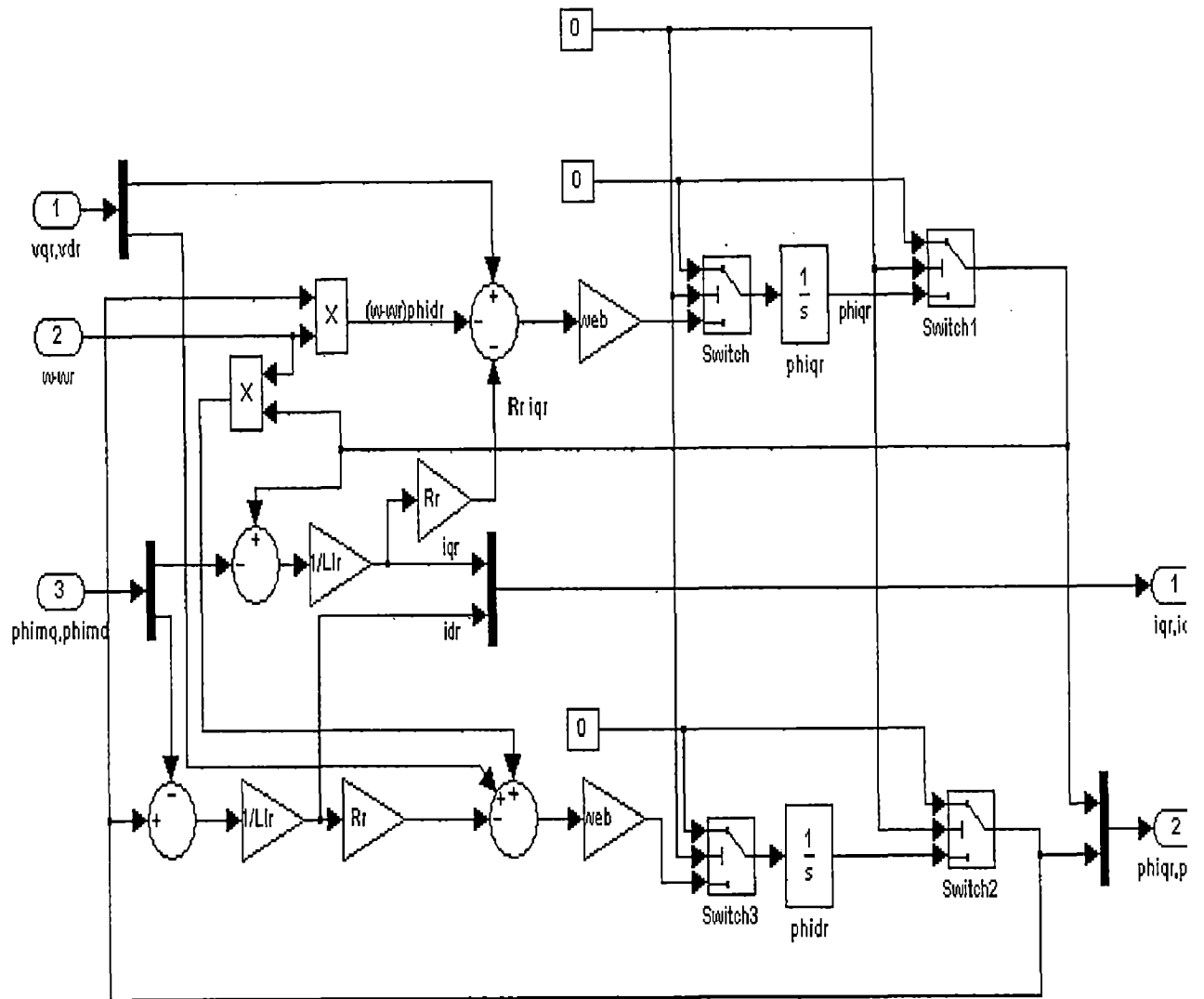
Fig. A.14   Model of rotor side dq current and flux.
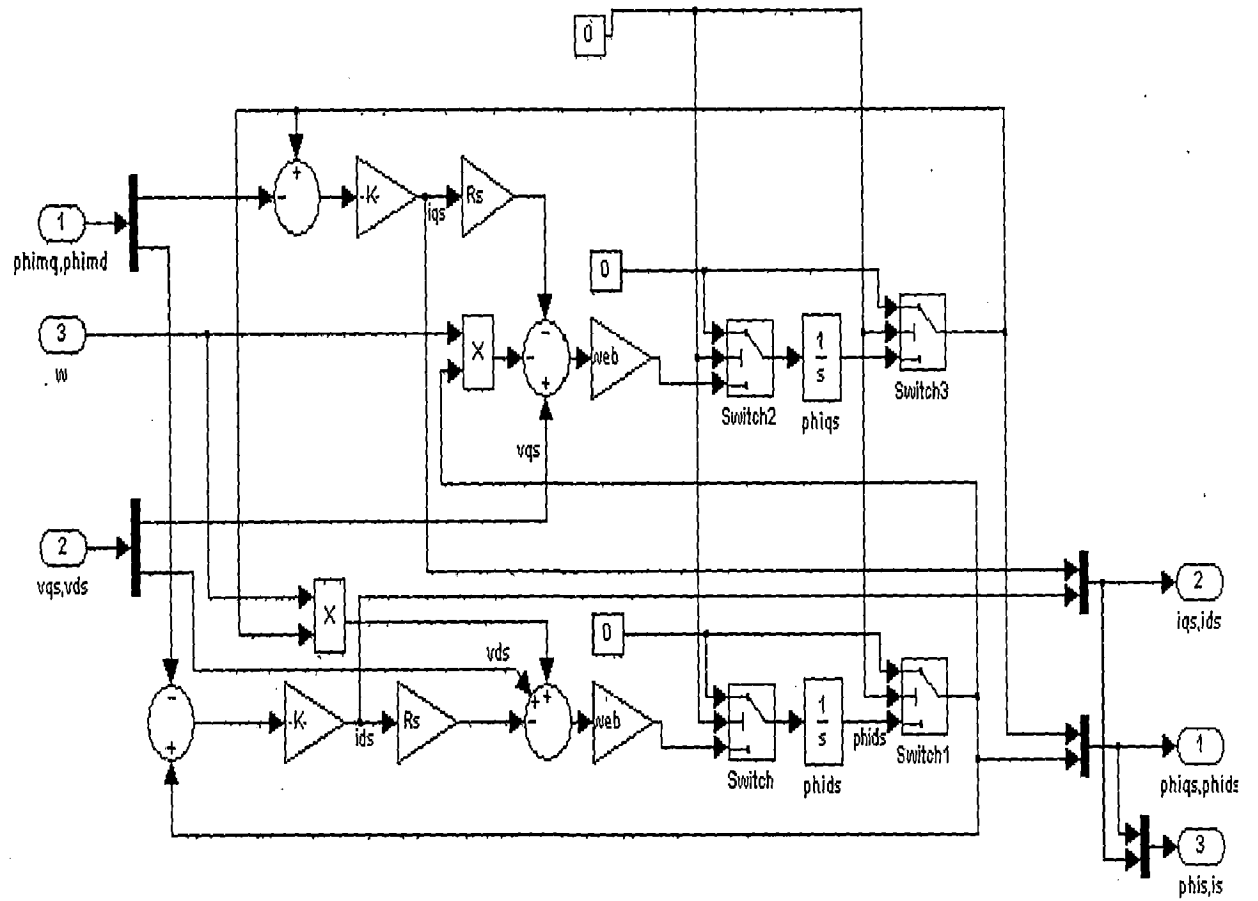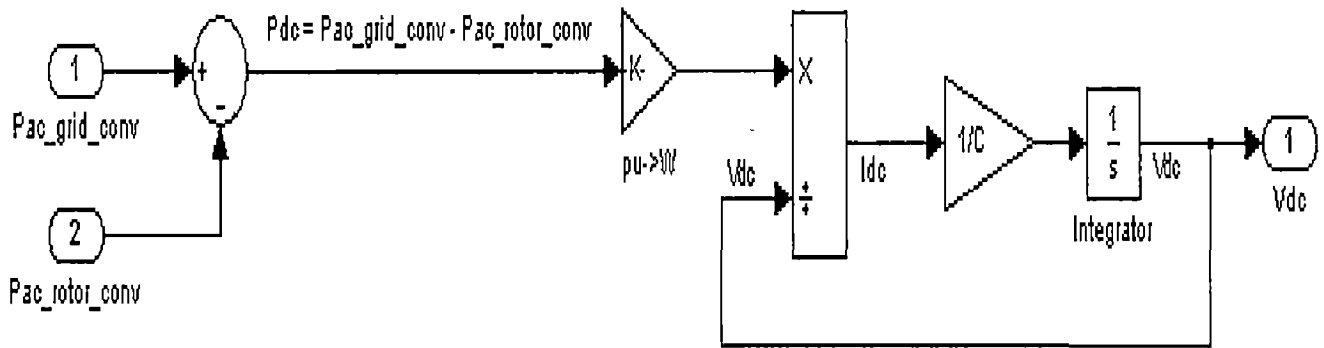
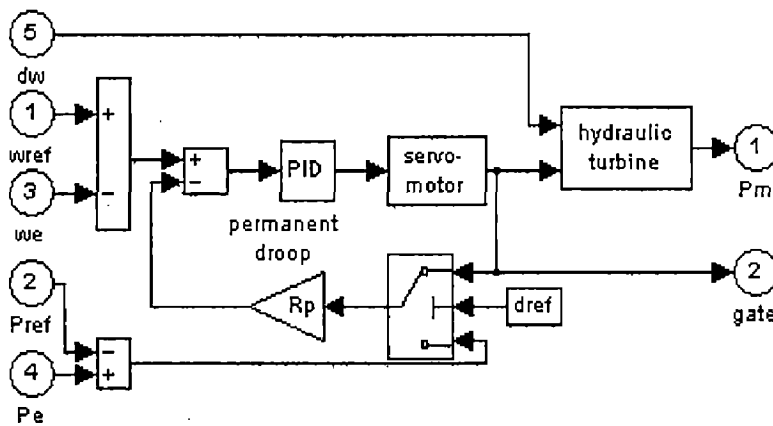Fig. A.17 Model of stator side dq current and flux.

Fig. A.18 DC bus model .

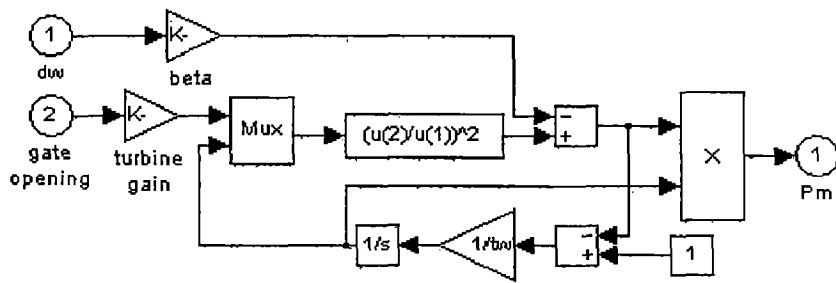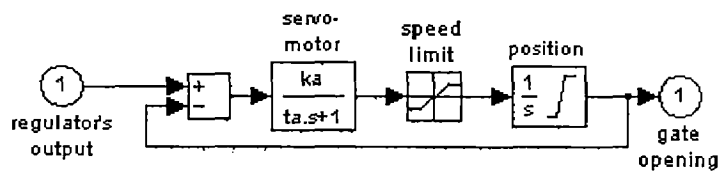Fig. A.19 Hydraulic Turbine Model

Fig. A.20 Sub blocks of hydraulic turbine

Fig. A.21 Sub blocks of Servo motor